the plant journal

SEB SOCIETY FOR EXPERIMENTAL BIOLOGY

The Plant Journal (2019) **100,** 969–990 doi: 10.1111/tpj.14490

AtERF#111/ABR1 is a transcriptional activator involved in the wounding response

Judith Bäumler[1], Willi Riber[1], Maria Klecker[1,2,3], Leon Müller[1], Nico Dissmeyer[2,3,†], Alfons R. Weig[4] and Angelika Mustroph[1,*]

[1]*Plant Physiology, University Bayreuth, Universitaetsstr. 30, 95440 Bayreuth, Germany,*
[2]*Independent Junior Research Group on Protein Recognition and Degradation, Leibniz Institute of Plant Biochemistry, Weinberg 3, 06120 Halle (Saale), Germany,*
[3]*Science Campus Halle – Plant-Based Bioeconomy, Betty-Heimann-Str. 3, 06120 Halle (Saale), Germany, and*
[4]*Genomics & Bioinformatics, University Bayreuth, Universitaetsstr. 30, 95440 Bayreuth, Germany*

Received 10 July 2019; revised 24 July 2019; accepted 29 July 2019; published online 6 August 2019.
*For correspondence (e-mail angelika.mustroph@uni-bayreuth.de).
†Present address: Chair of Plant Physiology, University of Osnabrück, Barbarastr. 11, 49076 Osnabrück, Germany

SUMMARY

AtERF#111/ABR1 belongs to the group X of the ERF/AP2 transcription factor family (GXERFs) and is shoot specifically induced under submergence and hypoxia. It was described to be an ABA-response repressor, but our data reveal a completely different function. Surprisingly, *AtERF#111* expression is strongly responsive to wounding stress. Expression profiling of *ERF#111*-overexpressing (OE) plants, which show morphological phenotypes like increased root hair length and number, strengthens the hypothesis of AtERF#111 being involved in the wounding response, thereby acting as a transcriptional activator of gene expression. Consistent with a potential function outside of oxygen signalling, we could not assign AtERF#111 as a target of the PRT6 N-degron pathway, even though it starts with a highly conserved N-terminal Met–Cys (MC) motif. However, the protein is unstable as it is degraded in an ubiquitin-dependent manner. Finally, direct target genes of AtERF#111 were identified by microarray analyses and subsequently confirmed by protoplast transactivation assays. The special roles of diverse members of the plant-specific GXERFs in coordinating stress signalling and wound repair mechanisms have been recently hypothesized, and our data suggest that AtERF#111 is indeed involved in these processes.

Keywords: ERF/AP2 transcription factors, PRT6 N-degron pathway, hypoxia, submergence, wounding, abscisic acid, *Arabidopsis thaliana*.

INTRODUCTION

During their life cycle, plants are continuously subjected to an immense number of abiotic (e.g. too much or too little water, salt, cold, heat) and biotic (e.g. pathogenic bacteria, insects, fungi) stress factors that impair growth, development and reproduction. Due to a changing climate, the number of heavy rainfalls and floods has markedly increased in recent decades, impacting dramatically plant performance (Bailey-Serres *et al.*, 2012). Model-based large-scale projections predict a four-fold increase in flood hazards in most areas of the world by the end of this century (Hirabayashi *et al.*, 2008, 2013; Alfieri *et al.*, 2017). Submergence of plants caused by flooding events leads to restricted gas diffusion between the plant and its environment. Consequently, the gaseous plant hormone ethylene accumulates, whereas a shortage in O_2 and CO_2 limits aerobic respiration as well as photosynthesis, resulting in a severe energy crisis and carbohydrate deficit (Bailey-Serres and Voesenek, 2008; Sasidharan *et al.*, 2018).

As sessile organisms, plants rely on faithful perception of the low-oxygen stress (hypoxia) and have to timely translate it into adaptive responses by reprogramming gene expression and transcriptional regulation. In *Arabidopsis thaliana,* oxygen sensing is achieved by the homeostatic regulation of the stability of the Ethylene Response Factor family (ERF), subgroup VII (GVIIERFs) transcription factors via the Cys branch of the PRT6 N-degron pathway of ubiquitin-mediated proteolysis (Gibbs *et al.*, 2011, 2014; Licausi *et al.*, 2011; Dissmeyer, 2019). The five GVIIERFs – RELATED TO APETALA2.2 (RAP2.2), RAP2.3, RAP2.12, HYPOXIA-RESPONSIVE ERF1 (HRE1) and

HRE2 – are characterized by a highly conserved N-terminal MCGGAI(I/L) motif (amino acid single letter code), whose second amino acid cysteine (Cys2) determines their stability dependent on the availability of molecular oxygen and nitric oxide (NO). In brief, METHIONINE AMINOPEPTIDASES 1 and 2 (MAP1/2) constitutively expose an N-terminal Cys2 by removal of the initiator methionine (Met1). An oxidation of Cys2 by plant cysteine oxidases (PCOs) (Weits *et al.*, 2014; White *et al.*, 2017, 2018) makes the protein accessible for further modifications catalyzed by ARGINYL-tRNA PROTEINTRANSFERASES (ATEs) (White *et al.*, 2017) and the downstream acting E3 Ub ligase PROTEOLYSIS6 (PRT6), which is suggested to poly-ubiquitinate the protein and mark it for degradation by the 26S proteasome (Gibbs *et al.*, 2011; Licausi *et al.*, 2011; summarized in Dissmeyer, 2019). In contrast, hypoxic conditions or an inhibition of NO accumulation are sufficient for the stabilization of the GVIIERFs, which control the transcription of hypoxia-responsive genes (HRGs) by binding to the 12 base pairs (bp) long hypoxia-responsive promoter element (HRPE) (Bui *et al.*, 2015; Gasch *et al.*, 2016).

In Arabidopsis, 122 ERF genes, divided into 12 subgroups (I–X, VI-L and Xb-L), were identified (Nakano *et al.*, 2006). These plant-specific transcription factors share an APETALA2 (AP2) DNA binding domain and have various functions during developmental and physiological processes in plants. Aside from the GVIIERFs, more than 200 proteins in the Arabidopsis genome initiate with Met–Cys (MC), making them potential PRT6 N-degron pathway substrates. Among these, the transcription factor (TF) AtERF#111, ABSCISIC ACID REPRESSOR 1 (ABR1), gained our interest. AtERF#111 is one of eight members of the subgroup X of the ERF/AP2 family (Nakano *et al.*, 2006). Recently, two other proteins with an N-terminal MC motif, VERNALISATION2 (VRN2) (Gibbs *et al.*, 2018) and LITTLE ZIPPER 2 (ZPR2) (Weits *et al.*, 2019) were demonstrated to be oxygen-sensitive targets of the Cys branch of the PRT6 N-degron pathway, thereby linking oxygen availability to the epigenetic control of plant development and shoot meristem activity, respectively.

PRT6 N-degron pathway mutants have been described to show altered ABA sensitivity (Holman *et al.*, 2009; Gibbs *et al.*, 2014). Among these, *ged1*, a mutant defective in *PRT6*, as well as *prt6-1* and the double mutant *ate1 ate2*, exhibited enhanced sensitivity to ABA during germination (Holman *et al.*, 2009). Also, microarray analysis of *ged1* showed downregulation of ABA-responsive genes already upon control conditions (Choy *et al.*, 2008; Riber *et al.*, 2015). Interestingly, *AtERF#111* was suggested to be induced upon drought stress and involved in ABA signalling (Pandey *et al.*, 2005; Ha *et al.*, 2014). In addition, the expression of *AtERF#111* was induced upon hypoxia and submergence (Tsai *et al.*, 2014; van Veen *et al.*, 2016; Yeung *et al.*, 2018). However, knowledge of *AtERF#111* expression under different stress conditions was very limited so far due to the lack of this sequence on the widely used Affymetrix ATH1 microarray chip.

Here we show that *AtERF#111* is shoot specifically induced upon submergence and hypoxia. Even though AtERF#111 starts with an N-terminal MC motif, we could not confirm its degradation by the PRT6 N-degron pathway. Nevertheless, protein stability experiments showed ubiquitin-dependent degradation. AtERF#111 was described to be an ABA-response repressor (Pandey *et al.*, 2005), but our data suggest a completely different function. We could not confirm an involvement of AtERF#111 in ABA signalling or the drought response. However, we revealed a strong induction of *AtERF#111* upon wounding. A microarray analysis of *AtERF#111*-overexpression (OE) plants showed a pronounced overlap between genes induced by *AtERF#111* and by wounding. Interestingly, *AtERF#111*-OE led to a clear phenotype in root hair length and number which correlates with the *AtERF#111* transcript level. We were able to identify direct target genes of AtERF#111 using a glucocorticoid-inducible protoplast assay, which also showed a link to wounding stress.

RESULTS

The expression of *AtERF#111* is induced upon hypoxia and submergence

Earlier expression analyses on plants under hypoxia or submergence did not contain information on *AtERF#111* (AT5G64750) expression. However, new technologies such as RNA-seq as well as the use of the Agilent Arabidopsis 4×44k chip have revealed interesting expression patterns of this gene. The expression of *AtERF#111* was shown to be induced during submergence in datasets of RNA-seq as well as ribosome sequencing (van Veen *et al.*, 2016; Yeung *et al.*, 2018). In detail, the RNA-seq data analysis was performed after 4 h of submergence in darkness and indicated a shoot-specific upregulation of *AtERF#111* in all eight tested Arabidopsis accessions (Figure S1). Therefore, we analyzed the *AtERF#111* transcript level by RT-qPCR after 24 h of submergence of 3-week-old plants and could confirm an induction of *AtERF#111* already upon dark treatment (AD) in comparison with illuminated control conditions (AL), as well as an increased induction by the compound stress of darkness and submergence (SD) (Figure 1).

In addition to that, we analyzed the *AtERF#111* transcript level in hypoxia-stressed seedlings within a time course experiment. The expression of *AtERF#111* was significantly induced after 8 h of hypoxia treatment and remained upregulated after 1 h of re-aeration (both in light) (Figure 1b). When separating roots and shoots of hypoxia-treated seedlings, we could confirm a shoot-specific upregulation of *AtERF#111* (Figure S2). Interestingly, there

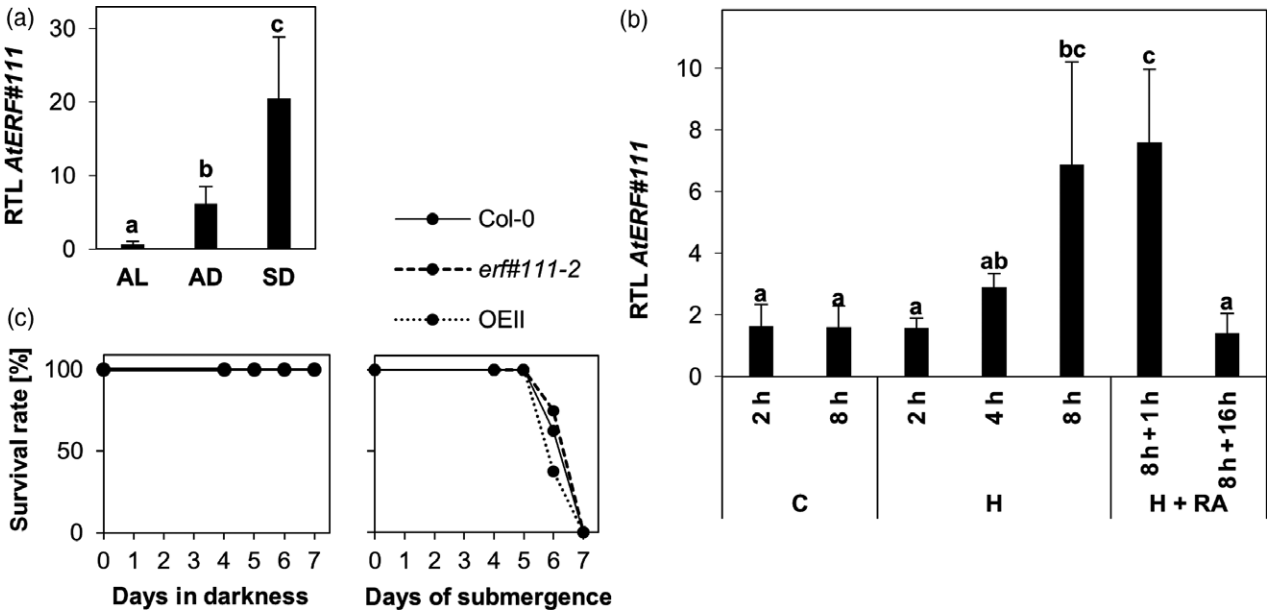

Figure 1. Analyses of *AtERF#111* expression upon hypoxia and submergence and submergence survival. (a) Arabidopsis plants were grown until the 10-leaf stage (8 h photoperiod). Two hours after the beginning of the photoperiod, plants were either kept under control conditions air + light (AL) or were transferred to air + darkness (AD) or to submergence + darkness (SD). After 24 h, leaf material (except cotyledons) was harvested (two plants were pooled per treatment). Values are means ± SD from three biological replicates. Different letters indicate values that vary significantly at $P < 0.05$ (one-way ANOVA, Tukey honest significant difference (HSD) test). (b) RT-qPCR analysis of *AtERF#111* relative transcript levels (RTL) in 7-day-old WT seedlings, treated with hypoxia (H) for 2, 4, or 8 h (in light) and 8 h followed by 1 or 16 h of re-aeration (RA). Controls (C) were kept under normoxic conditions. Transcript levels were normalized to *ELONGATION FACTOR 1A* (*EF1a*) mRNA. Values are means ± SD from three biological replicates (each with three technical replicates). Different letters indicate values that vary significantly at $P < 0.05$ (one-way ANOVA, Tukey HSD test). (c) Plants (10-leaf stage) were submerged in darkness for 4, 5, 6 or 7 days. Controls were kept in dark and air for the same time. After 2 weeks of recovery under short-day conditions, the survival rate of the plants was scored, which was determined as the ability to form new leaves. Data of one experiment ($n > 8$) are shown (see Figure S5 for further replicates).

were no differences in *AtERF#111* transcript level when comparing wildtype (WT) Col-0 and the PRT6 N-degron pathway mutant *prt6-1*, indicating that the *AtERF#111* gene is not a target of the GVIIERFs. According to that, we could not identify any HRPE in the region comprising 3 kb upstream of the transcription start site by using the RSA tool *matrix-scan*.

To test whether an altered expression of the low-oxygen responsive *AtERF#111* had an impact on post-submergence survival, two T-DNA insertion lines were isolated, SALK_094151C (*erf#111-1*) and SALK_012151C (*erf#111-2*). As annotated (http://www.arabidopsis.org), we could confirm the T-DNA insertion of *erf#111-1* in the intron and of *erf#111-2* in the second exon by sequencing. Only for *erf#111-2*, no transcript was detected after hypoxia treatment, which therefore displays a true null allele, whereas the intronic T-DNA insertion of *erf#111-1* is most likely removed by splicing processes (Figure S3). Three-week-old plants of the *erf#111-2* mutant did not show an altered survival after short-term submergence under dark conditions (4–7 days), followed by 2 weeks recovery relative to Col-0 (Figures 1c and S4). Furthermore, we generated stable *AtERF#111*-OE Arabidopsis plants in the WT background, having an N-terminal His_6-FLAG epitope to mask AtERF#111 from potential degradation by the PRT6 N-degron pathway (see below, OEI and OEII). OEII only displayed a slightly decreased survival capacity after submergence in comparison with Col-0 and *erf#111-2*, but this could also be due to phenotypic differences of the OE lines already under normoxic conditions (see below).

AtERF#111 is not a target of the PRT6 N-degron pathway, but is degraded in an ubiquitin-dependent manner

As the N-terminus of AtERF#111 initiates with the amino acids MC, it represents a possible PRT6 N-degron pathway substrate. Interestingly, the N-terminal region (including the first eight amino acids) of AtERF#111 seems to be highly conserved in homologous proteins of different Brassicaceae species, for example *Arabidopsis lyrata*, *Arabidopsis halleri* or *Capsella rubella* (Figure S5). The GVIIERFs, however, show a motif at their N-terminus (consensus MCGGAI/L) which is different from the N-terminus of AtERF#111 and homologs. It was shown that a substitution of Cys with Ala is sufficient to inhibit protein degradation by the PRT6 N-degron pathway, leading to a stabilization of the GVIIERFs under normoxic conditions (Gibbs *et al.*, 2011, 2014). Therefore, constructs containing AtERF#111 with the natural (MC) and the mutated (MA) N-terminal residues were generated as fusion constructs with C-terminal epitope tags. In accordance with the function as

a TF, a localization of both AtERF#111 constructs fused with a C-terminal green fluorescent protein (GFP)-tag could be detected in the nucleus of transiently transformed tobacco leaves (Figure 2). As there was no clear difference in fluorescence intensity and therefore in protein stability of the two AtERF#111 versions, we performed a cycloheximide (CHX)-chase experiment in Arabidopsis WT protoplasts to evaluate protein stability *in vivo*. The CHX-chase assay showed that both (MC)AtERF#111 and (MA) AtERF#111 (fused with C-terminal haemagglutinin (HA)), disappeared independently of their N-termini within 3 h in the presence of the translational inhibitor CHX (Figure 2b). Therefore, under the tested conditions, AtERF#111 could not be assigned as a target of the PRT6 N-degron pathway. However, co-incubation with the 26S proteasome inhibitor MG132 clearly resulted in a stabilization of the AtERF#111 protein, and protein steady-state levels were markedly increased (Figure 2c). Hence, these results demonstrated that AtERF#111 – despite its N-terminal MC motif – does not seem to be a target of the PRT6 N-degron pathway, but is still a target of the 26S proteasome.

AtERF#111 does not repress the ABA response

Pandey *et al*. (2005) suggested for AtERF#111 a role as a repressor of ABA signalling, and therefore named it ABSCISIC ACID REPRESSOR 1 (ABR1). This hypothesis was based on experiments with two *erf#111* T-DNA insertion lines in the Col-0 background (SAIL140_G06 and SALK_012151C). In addition to an induction of *AtERF#111* expression upon cold, high salt and drought stress, an increase in transcript level upon ABA treatment as well as a higher transcript accumulation of selected ABA-marker genes in the mutant lines compared with the WT were observed. Furthermore, *erf#111* mutant lines showed a hypersensitive ABA-mediated response in comparison with the WT regarding seed germination at 0.7 μM ABA and root growth at 10 μM ABA.

We aimed at confirming these findings and to further evaluate the function of the TF. To that end, we used *erf#111-2* (SALK_012151C), one of the two T-DNA insertion lines analyzed by Pandey *et al*. (2005). Additionally, we made use of two His_6-FLAG-*AtERF#111*-OE lines (OEI and OEII) originating from independent T-DNA insertion events in the Col-0 background (see below). However, in our experiments we could not detect any differences between WT and *erf#111-2*, and the His_6-FLAG-OE lines showed contradicting results to AtERF#111 being an ABA repressor (Figure 3). In detail, we performed the germination assay with varying ABA concentrations (0–0.7 μM ABA) and only used seeds of the same age. The latter is very important, as the sensitivity towards ABA can alter with increasing seed age (Holman *et al*., 2009). The ability to germinate decreased with increasing ABA concentrations, to a comparable extend for WT and *erf#111-2* (Figure 3a). The OE lines showed partial yellowing of the cotyledons as well as uneven root lengths already under control conditions.

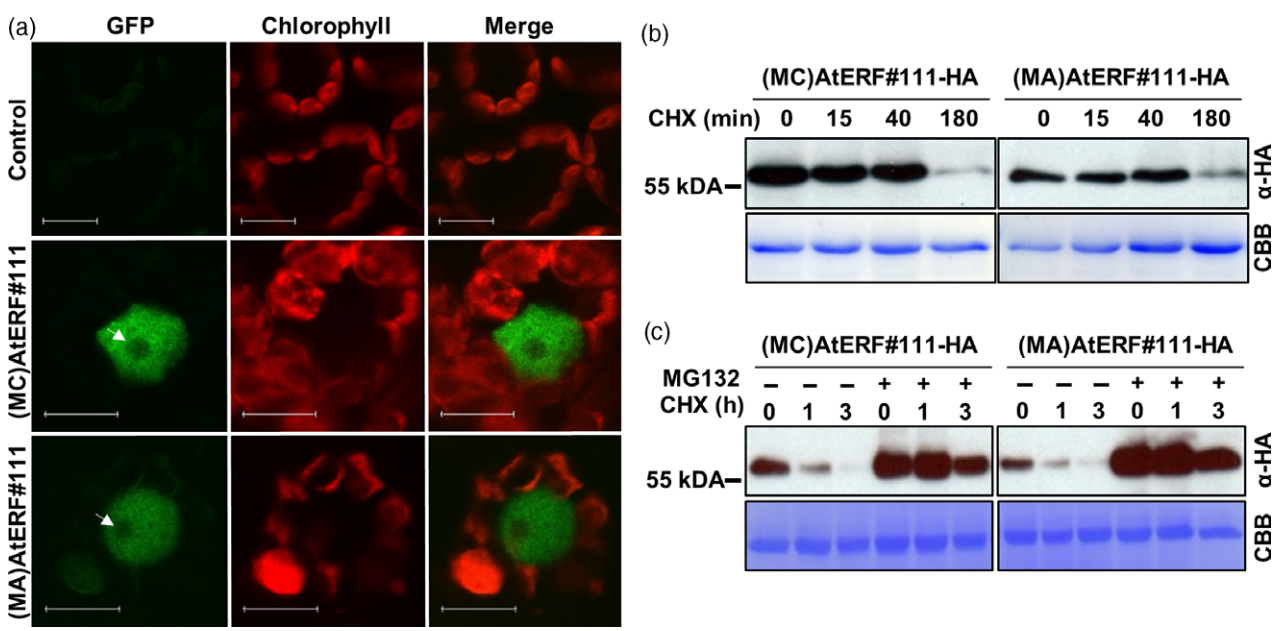

Figure 2. AtERF#111 is not a target of the PRT6 N-degron pathway, but is a target of the 26S-proteasome. (a) Confocal laser scanning microscopy visualization of tobacco plants transiently expressing p35S:(MC)AtERF#111-GFP and p35S:(MA)AtERF#111-GFP. Bar: 15 μm. White arrow indicates the nucleolus. Chlorophyll and GFP fluorescence and merged images of infiltrated tobacco leaves are shown. (b) Stability of AtERF#111 constructs with a modified N-terminus in Arabidopsis WT protoplasts. Protoplasts were either transfected with p35S:(MC)AtERF#111-HA or p35S:(MA)AtERF#111-HA and incubated with 100 μM cycloheximide (CHX) for the indicated time periods. Coomassie brilliant blue (CBB) staining was used as the loading control. The molecular weight of $AtERF\#111^{3HA}$ is 49 kDa. (c) CHX chase of p35S:(MC)AtERF#111-HA and p35S:(MA)AtERF#111-HA with or without the proteasome inhibitor MG132 (50 μM).

They did not display higher ABA insensitivity in comparison with Col-0, as one would expect if AtERF#111 was an ABA-response repressor. Similar results were obtained for the root growth assay: The root lengths decreased with increasing ABA concentrations, showing again no differences between *erf#111-2* and Col-0 (Figure 3b). At concentrations of 50 and 100 μM ABA, the OE lines displayed shorter roots than the WT.

To verify the effectiveness of our ABA treatment, we repeated these two assays including the published ABA hypersensitive mutant *prt6-1* (Holman *et al.*, 2009) as well as the ABA insensitive quadruple mutant of the ABA receptors pyrabactin resistance1/PYR1-like (PYR1/PYL) *pyr1 pyl1 pyl2 pyl4* (Park *et al.*, 2009) (Figures S6 and S7). To compare these mutants to Col-0 and *erf#111-2*, germination was assessed in more detail and scored into different categories with the criteria of no visible radicle protrusion (=dead), visible radicle protrusion (>1 mm length) as well as full seedling establishment (including the formation of green cotyledons) (Figure S6). Indeed, *prt6-1* displayed hypersensitive inhibition of germination in comparison with Col-0 and was not able to establish green cotyledons at any ABA concentration tested, whereas *pyr1 pyl1 pyl2 pyl4* was ABA insensitive and showed full seedling establishment even at 0.7 μM ABA. In contrast with these lines, *erf#111-2* behaved similar to Col-0 and showed an intermediate phenotype with 6–12 % of dead seeds and about 80–90% visible radicle protrusions at 0.7 μM ABA.

Regarding the root growth assay, the quadruple mutant *pyr1 pyl1 pyl2 pyl4* displayed a higher relative root length as well a significantly increased relative seedling weight than Col-0, whereas there were no detectable differences between Col-0, *erf#111-2* and *prt6-1* (Figure S7). The latter was expected, as Holman *et al.* (2009) reported that *prt6* alleles show an ABA hypersensitivity of germination, but not a hypersensitivity regarding ABA inhibition of root elongation. Therefore, these data confirmed again our findings that *erf#111-2* shows no modified ABA sensitivity in comparison with Col-0.

Furthermore, the ABA-responsive genes *ARABIDOPSIS THALIANA DROUGHT-INDUCED 8*/*RESPONSIVE TO ABA 18* (*ATDI8*/*RAB18*; *AT5G66400*) and *RESPONSIVE TO DESICCATION 22* (*RD22*; *AT5G25610*) did not show an altered expression between the *erf#111-2* mutant, WT and the OE lines after ABA treatment. Even the *AtERF#111* expression itself did not increase in response to ABA treatment in our hands (Figure 3c), as was reported by Pandey *et al.* (2005). These results are confirmed by transcriptome data from a time series RNA-seq experiment (Song *et al.*, 2016) as well as by microarray analysis (Liu *et al.*, 2013), which also displayed no differential expression of *AtERF#111* in response to ABA treatment. Consequently, under the conditions used here, our experiments show that AtERF#111 is not involved in ABA signalling and therefore is no ABA repressor.

AtERF#111 is not induced by drought, but strongly induced by wounding stress

Microarray data by Ha *et al.* (2014) implied an induction of *AtERF#111* expression in response to drought stress (Gene Expression Omnibus (GEO) accession no.: GSE48949). In that experiment, the aerial parts of 24-day-old plants were detached and exposed to dehydration on paper for 0 (control), 2 and 4 h. However, microarray data by Nishiyama *et al.* (2013) did not show an effect of drought stress on the expression of *AtERF#111* (GEO accession: GSE42290). In the corresponding experiment, 3-week-old plants were grown in pots for 10 days without watering or grown under well watered conditions (control). These contradictory findings led us to repeat the different drought treatments. Firstly, when we subjected plants (8 leaf stage) to drought stress by letting them grow in pots for 9 days without watering, we observed a >250-fold induction of the drought-induced marker gene *AtRAB18* in comparison with control plants by RT-qPCR (Figure 4; Figure S8). However, *AtERF#111* showed no changes in transcript level in accordance with the data from Nishiyama *et al.* (2013). Secondly, when we exposed whole plants (8 leaf stage) to dehydration on papers for 3 h, *AtRAB18* expression increased 30-fold in comparison with controls in soil. This time, also *AtERF#111* showed a 75-fold induction of expression. Of note, while Ha *et al.* (2014) only detached the aerial parts, we chose to place the whole plants including roots onto paper. Importantly, this experimental setup did not interfere with the induction of *AtERF#111* expression, as similar induction was observed in the shoots of plants when exposed to dehydration on paper with or without the roots (Figure S9). Consequently, we could also confirm the data from Ha *et al.* (2014).

However, given the artefact-prone stress treatment applied by Ha *et al.* (2014), we decided to introduce another control treatment, in which we covered the roots of the exposed plants with wet paper to avoid dehydration. Surprisingly, *AtERF#111* expression increased under these conditions to the same amount as without moistening, whereas *AtRAB18* expression did not alter between controls in pots and controls on papers (Figure 4a). Hence, we hypothesized that just removing the plant from the soil is sufficient to induce *AtERF#111* expression, likely to be caused by wounding stress. To verify this assumption, we performed an independent time-resolved wounding experiment by slightly injuring the leaves with a needle and revealed that *AtERF#111* expression is strongly induced by this treatment (Figure 4b). In detail, its expression reached a maximum (>300-fold increase) 1 h after wounding stress and decreased to basal levels after 6 h.

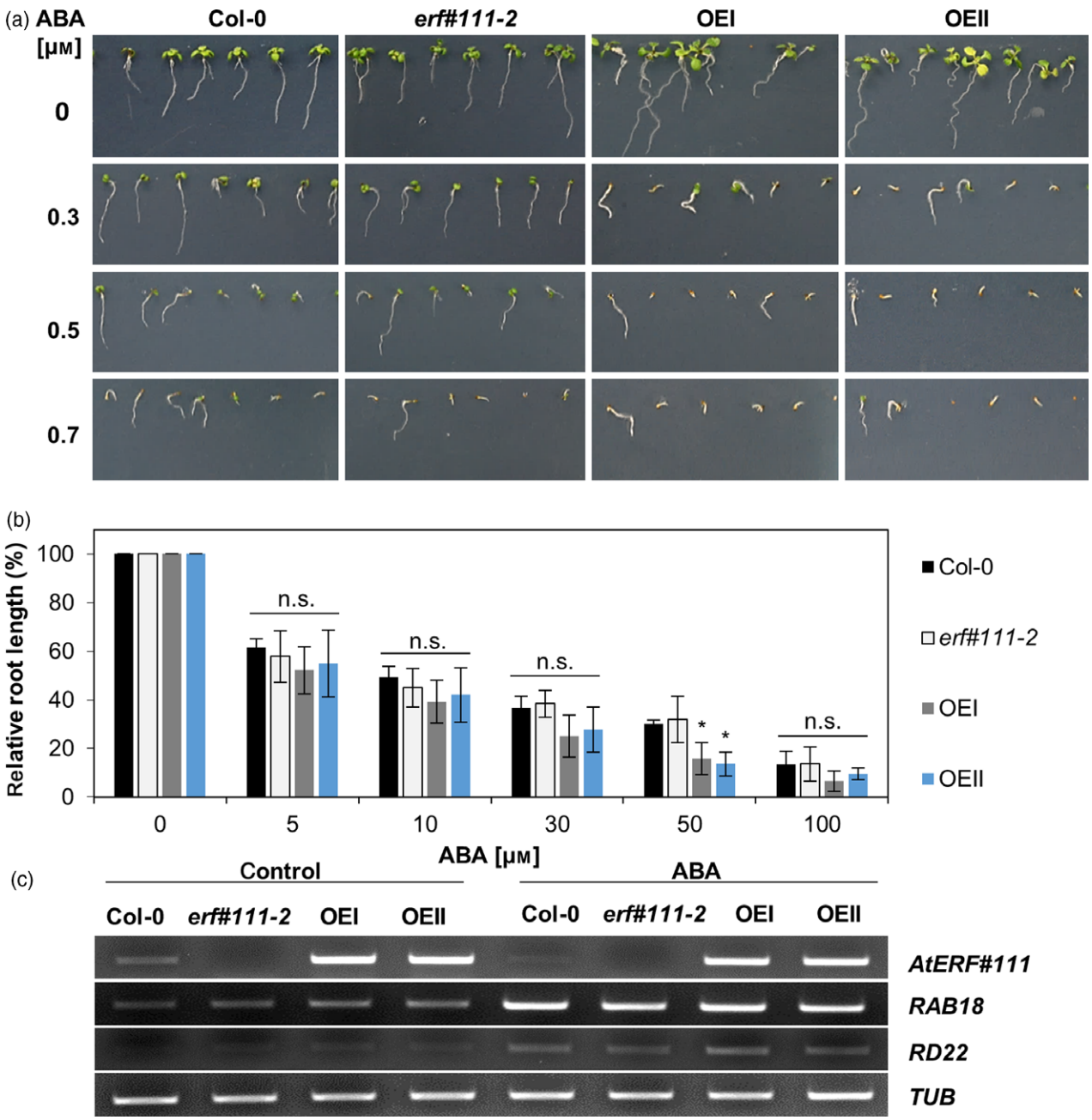

Figure 3. AtERF#111 is not involved in ABA signalling. (a) Germination assay in the presence of ABA. Seeds of the same age of Col-0, *erf#111-2*, *ERF#111*-OEI and *ERF#111*-OEII were placed on MS agar plates with different ABA concentrations (0–0.7 µM). The ability of germination was documented after 10 days (16 h photoperiod). Representative pictures of at least three biological replicates are shown. (b) Root growth assay in the presence of ABA. Three-day-old seedlings of Col-0, *erf#111-2*, OEI and OEII were placed on MS agar plates with different ABA concentrations (0–100 µM). After additional 14 days, the root length was measured. Relative root lengths are shown as the percentage of control plants. Values are means ± SD from the mean values of at least three biological replicates ($n > 10$ per replicate and treatment). The asterisks (*) indicate values that vary significantly at $P < 0.05$ (one-way ANOVA, Tukey HSD test) in comparison with Col-0 at each ABA concentration. n.s., not significant. (c) Expression analysis of the ABA-responsive genes *RAB18* and *RD22* after ABA treatment. Standard RT-PCR analysis of 7-day-old seedlings, sprayed with 100 µM ABA for 4 h. Control plants were equally treated with water. Representative results of three biological replicates are shown. *TUBULIN* (*TUB*) expression was used as a reference.

In addition, we generated stable Arabidopsis transgenics expressing firefly luciferase under control of the promoter of *AtERF#111* (prAtERF#111:fLUC in pBGWL7). At 90 min after wounding, bioluminescence could only be observed in leaves of prAtERF#111:fLUC lines, and importantly, the signal was restricted to the wounded sites (Figure 5). In contrast, no signal was observed in leaves of Col-0, confirming a wounding-dependent response of prAtERF#111 in leaves (Figure 5).

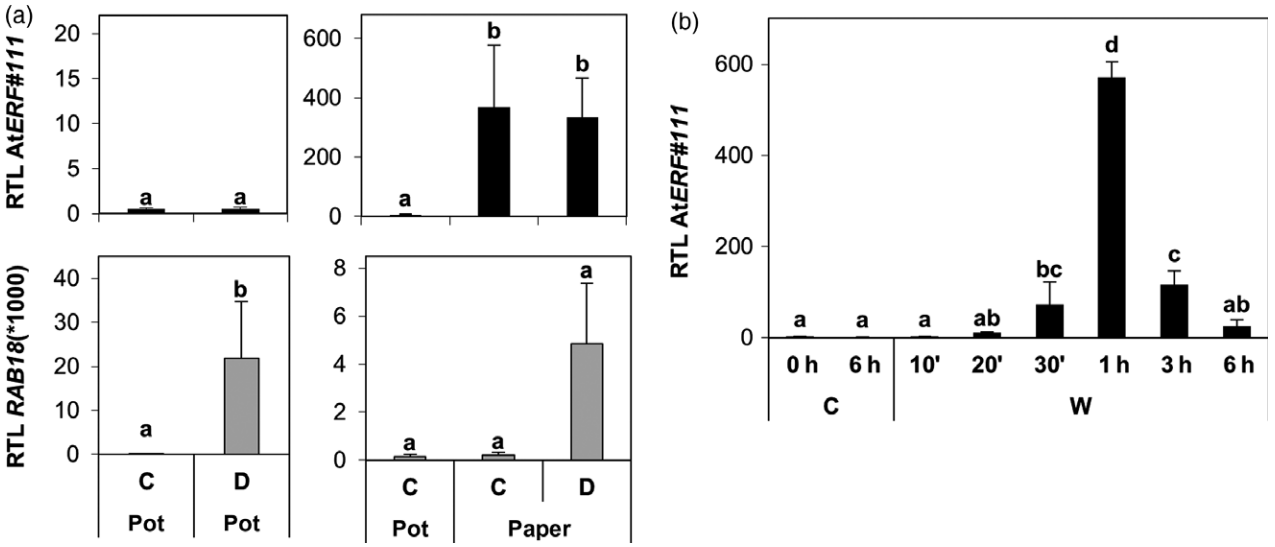

Figure 4. The expression of *AtERF#111* is not induced by drought but strongly induced by wounding stress. (a) RT-qPCR analyses of *AtERF#111* (black bars) and *RAB18* (grey bars) relative transcript levels (RTL) in stressed WT plants. Plants at the 8-leaf-stage (8 h photoperiod) were either exposed to drought stress (D pot) by letting them grow for 9 days without watering, whereas controls (C) were well watered (=C pot), or were exposed to dehydration on papers for 3 h, whereas the roots of the control plants were covered with wet paper (=C/D paper). (b) The leaves of 3-week-old plants were gently wounded with a needle. Plant material was harvested after different time points (10, 20 and 30 min and 1, 3 and 6 h), controls were harvested at the start (0 h) and the end of the treatment (6 h). Transcript levels were normalized to *ELONGATION FACTOR 1A* (*EF1a*) mRNA. (a, b) Values are means ± SD from three biological replicates (each with three technical replicates regarding the RT-qPCR). Different letters indicate values that vary significantly at $P < 0.05$ (*T*-test for the comparison of two means; one-way ANOVA and Tukey HSD test for the comparison of more than two means).

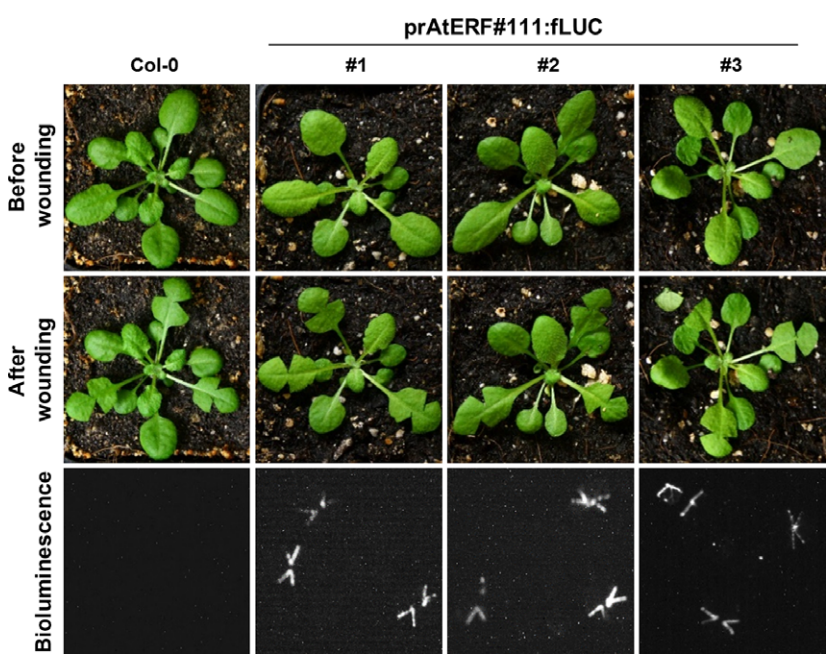

Figure 5. Wounding-dependent accumulation of prATERF#111:fLUC fusions. Stable *A. thaliana* lines expressing the *AtERF#111* promoter (1302 bp) and a fLUC coding sequence (prAtERF#111:fLUC). Wounding-dependent bioluminescence after application of 2 mM D-luciferin + 0.1% (v/v) Triton X-100 was only seen in leaves of plants expressing prAtERF#111:fLUC 90 min after wounding, whereas no signal was observed in leaves of Col-0. Pictures of bioluminescence were taken in a low-light imaging system (Intas, Göttingen, Germany) with a camera shutter time of 20 min.

Analysis of *AtERF#111* expression upon other stress treatments

As we could observe an induction of *AtERF#111* upon hypoxia, submergence and upon wounding, we wanted to evaluate other related stress conditions. When plants are flooded, they rapidly accumulate high levels of ethylene – a volatile plant hormone that triggers further signalling cascades (Sasidharan *et al.*, 2018). However, we could not detect a change in *AtERF#111* transcript levels after spraying 7-day-old seedlings with the ethylene precursor 1-aminocyclopropane-1-carboxylic acid (ACC) (Figure 6). Methyl jasmonate (MeJA) induces wound-responsive gene expression in plants and also H_2O_2 is systemically

generated in leaves upon wounding stress (León *et al.*, 2001). We could observe a 2.1-fold induction of *AtERF#111* expression by H_2O_2 treatment and a 3.6-fold induction by MeJA treatment. These findings endorse an involvement of AtERF#111 in the wounding response (Figure 6). Once again, we could not detect an *AtERF#111* induction upon ABA treatment in the context of this experiment (Figure 6, see also Figure 3c).

ERF#111-overexpression lines show differences in root and shoot development

We generated stable *ERF#111*-OE plants with an N-terminal His_6-FLAG epitope in the WT background to further investigate the function of the TF. Interestingly, *ERF#111*-OE lines displayed noticeable phenotypes. Here, 5-week-old plants (8 h light regime) possessed smaller leaves and petioles than the WT and often produced only a small amount of seeds (Figure 7). At the seedlings stage, His_6-FLAG-*ERF#111* overexpression significantly increased elongation and production of root hairs in comparison with Col-0 (Figure 7b,c). Using standard RT-PCR we analyzed, whether there was a correlation between root hair formation and *AtERF#111* transcript level of different *ERF#111*-OE lines. Therefore, we used nine OE lines derived from independent transformation events, and grouped them according to their number and length of root hairs. Strikingly, we could identify a clear positive correlation between root hair formation and transcript level: OE lines that formed only relatively little root hairs like Col-0 showed also only a low level of *AtERF#111* transcript, whereas its expression increased with increasing length and density of root hairs (Figure 7d). Based on the root hair phenotype, we chose the two lines OEI and OEII for further experiments, with the latter having longer root hairs than OEI and the strongest *AtERF#111* transcript level of various tested OE lines.

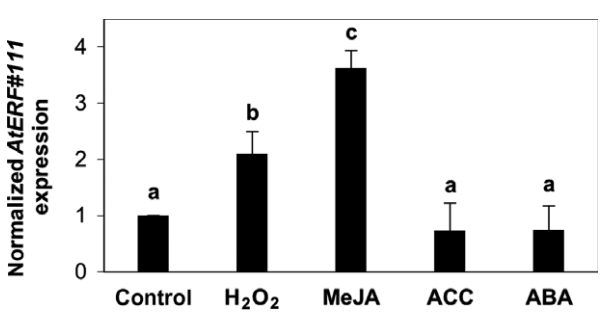

Figure 6. Expression analysis of *AtERF#111* upon various stress treatments. 7-day-old WT seedlings were sprayed with 10 mM H_2O_2, 50 μM MeJA, 500 μM ACC, or 100 μM ABA. *AtERF#111* transcript levels were analyzed relative to *ELONGATION FACTOR 1A* (*EF1a*) mRNA by RT-qPCR analyses and normalized to control treatments of the solvents (e.g., ethanol or water). For each treatment 0.01% Tween-20 was added. Values are means ± SD from three biological replicates (each with three technical replicates). Different letters indicate values that vary significantly at $P < 0.05$ (one-way ANOVA, Tukey HSD test).

In addition to that, we made cross-sections of the roots of 7-day-old seedlings to analyze the cell patterning of the rhizodermis. Normally, crucifers like Arabidopsis form root hairs in a position-dependent pattern: cells destined to become root hair cells (trichoblasts) have contact to two cortical cells, known as the hair position (H), whereas non-hair cells (atrichoblasts) only have contact to one cortical cell, which is the so-called non-hair position (N) (Dolan *et al.*, 1994). Interestingly, microtome sections of *ERF#111*-OE lines showed root hairs that were not only produced in root hair cell position, but also in the non-hair cell position, which normally does not produce root hairs (Figure 7e). As expected, WT seedlings only formed root hairs in the hair positions.

Gene expression profiling of *ERF#111*-overexpressing plants

We investigated the effect of *ERF#111*-OE on global gene expression by microarray profiling using the Arabidopsis 4×44k array (Agilent Technologies, Waldbronn, Germany). We harvested roots and shoots of 7-day-old His_6-FLAG-*ERF#111*-OEI and -OEII seedlings separately and compared gene expression data to roots and shoots of WT seedlings. We identified 807 differentially expressed genes (DEGs), whose transcript expression significantly varied more than two-fold in comparison with WT samples (|Signal-Log2-Ratio (SLR)| > 1, $P < 0.01$, Figure 8, Data S1). Here, 450 of the 807 DEGs were significantly upregulated by *ERF#111*-OE. Of these, 277 genes were only upregulated in shoots, 116 genes only in roots, and 57 genes in both shoots and roots. Furthermore, 357 of the 807 DEGs were significantly downregulated, 128 genes only in shoots, 222 in roots and seven in both shoots and roots.

When we compared all upregulated genes to the set of 49 core HRGs (Mustroph *et al.*, 2009) in order to test for a possible link to the anaerobic response, we could identify only one core gene, *RHODANESE* (*AT2G17850*) that was upregulated by *ERF#111*-OE in roots and shoots, and four more hypoxia core genes that were only upregulated in the shoots: two wound-responsive family proteins (*AT4G33560*, *AT4G10270*), *PYRUVATE DECARBOXYLASE 1* (*PDC1*, *At4G33070*) and *ETHYLENE RESPONSE2* (ETR2, *AT3G23150*). When comparing all DEGs with a SLR > 1 to microarray data from Arabidopsis seedlings that were submerged for 6 h in the dark (Hsu *et al.*, 2013), or subjected to 4 h anoxia (Tsai *et al.*, 2014), we could identify especially shoot-specific overlaps between the data sets (Figures 8b and S10). The overlaps between all *ERF#111*-OE shoot-induced genes and the submergence and anoxia treatment were calculated as statistically significant and therefore greater than expected by chance ($P < 0.001$, Fishers exact test), indicating a possible link to submergence and hypoxia. The hypoxia core gene *RHODANESE* was upregulated in all data sets.

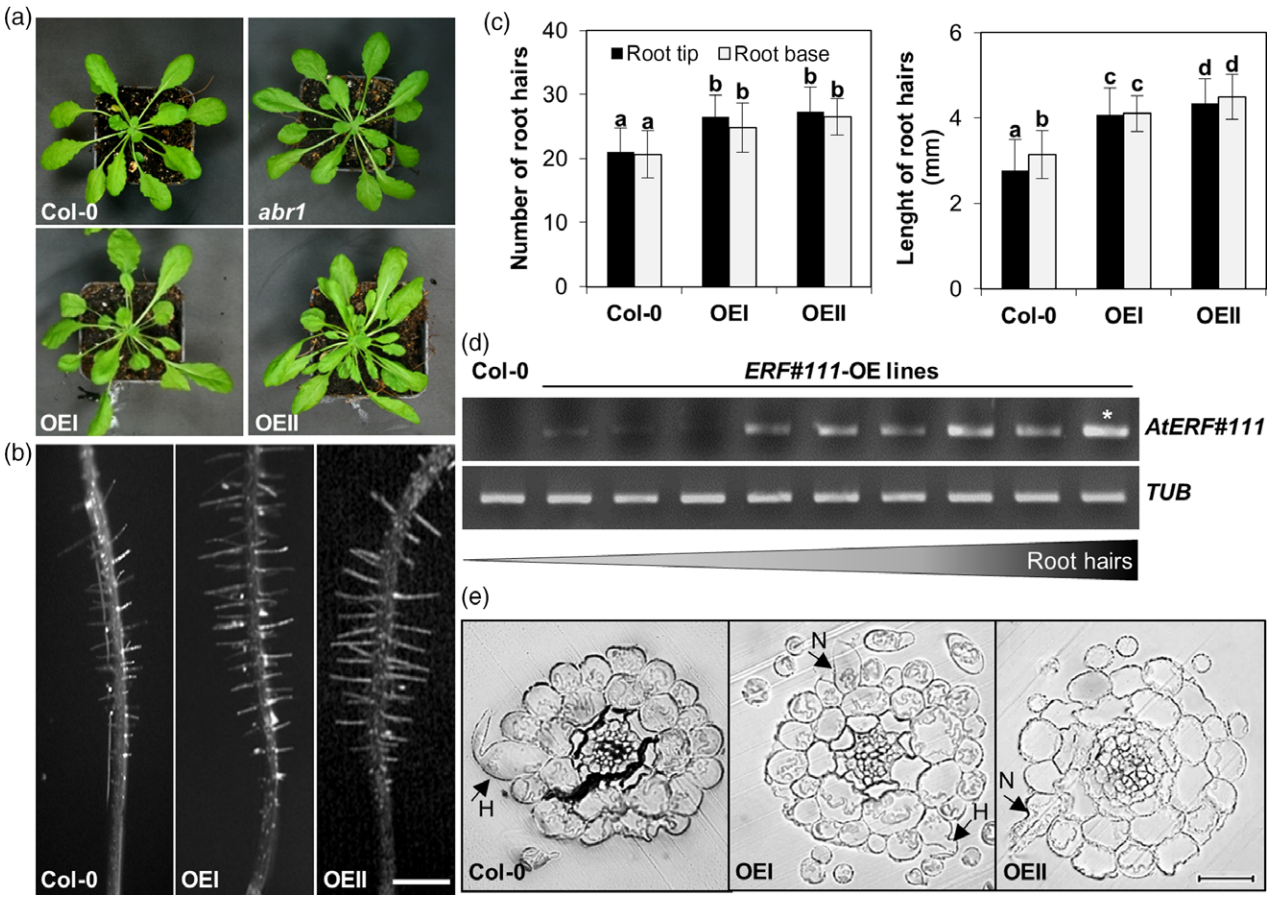

Figure 7. Phenotypes of *ERF#111*-overexpression lines. (a) Five-week-old plants (8 h photoperiod) of *ERF#111*-OE lines have smaller and more rosette leaves in comparison with Col-0. (b) Seven-day-old seedlings of *ERF#111*-OE plants show an increased root hair formation in comparison with Col-0. Bar: 0.5 mm. (c) Length ($n > 130$) and number of root hairs ($n > 14$) were determined at the root tip (black bars) and root base (grey bars). Values are means ± SD from two biological replicates. Different letters indicate values that vary significantly at $P < 0.05$ (one-way ANOVA, Tukey HSD test). (d) Correlation between *AtERF#111*-transcript level and root hair formation. Standard RT-PCR analysis of 7-day-old seedlings of different *ERF#111*-OE lines and Col-0, sorted according to their number and length of root hairs (*= OEII). *TUBULIN* (*TUB*) expression was used as a reference. Representative results from three biological replicates are shown. (e) Representative pictures of microtome sections (15 μm) of roots from 7-day-old seedlings. Root hairs in the *ERF#111*-OE lines in comparison with Col-0 are not only produced in root hair cells (H), which have contact to two cortical cells, but also in the non-hair cells (N), which have only contact to one cortical cell. Bar: 25 μm.

The genes most strongly induced by *ERF#111*-OE in the shoots were the class *I PLANT DEFENSINS PDF1.2c* (*AT5G44430*; *SLR 6.9*), *PDF1.3* (*AT2G26010*; *SLR 6.5*), *PDF1.2b* (*AT2G26020*; *SLR 6.1*), and *PDF1.2a* (*AT5G44420*; *SLR 4.5*). Those transcripts showed no change in expression in response to submergence or anoxia (references from Figure 8). As *AtERF#111* expression is also highly induced upon wounding treatment (Figure 4b), we hypothesized that AtERF#111 might have a function in the defence/wounding response. Therefore, we compared our data with an already published microarray experiment employing the 4×44k array in which the expression was measured 3 h after wounding of Arabidopsis leaves (Wang *et al.*, 2015) (Figure 8b). Consistent with our data, the microarray data by Wang *et al.* (2015) also included an induction of *AtERF#111* expression upon wounding. Again, the overlap between the DEGs by *ERF#111*-OE and the wounding arrays were calculated as being statistically significant ($P < 0.001$, Fishers exact test). Especially the genes most highly induced by *ERF#111*-OE were also differentially expressed upon wounding, for example members of the plant defensins, but also *Thioredoxin H-type 8* (TH8; AT1G69880) or *Strictosidine synthase 3* (SS3; AT1G74000). Additionally, we used Gene Ontology (GO) analysis to find enriched GO categories (see Data S2). Most enriched GO terms were found in the shoot-specific DEGs in comparison with root-specific DEGs (Figure 8c), including the molecular functions peroxidase activity, oxidoreductase activity and strictosidine synthase activity as well as biological processes connected to external stimuli, for example response to chemical, stress, hormone, defence or response to other organism, supporting the idea of AtERF#111 being involved in the wounding response.

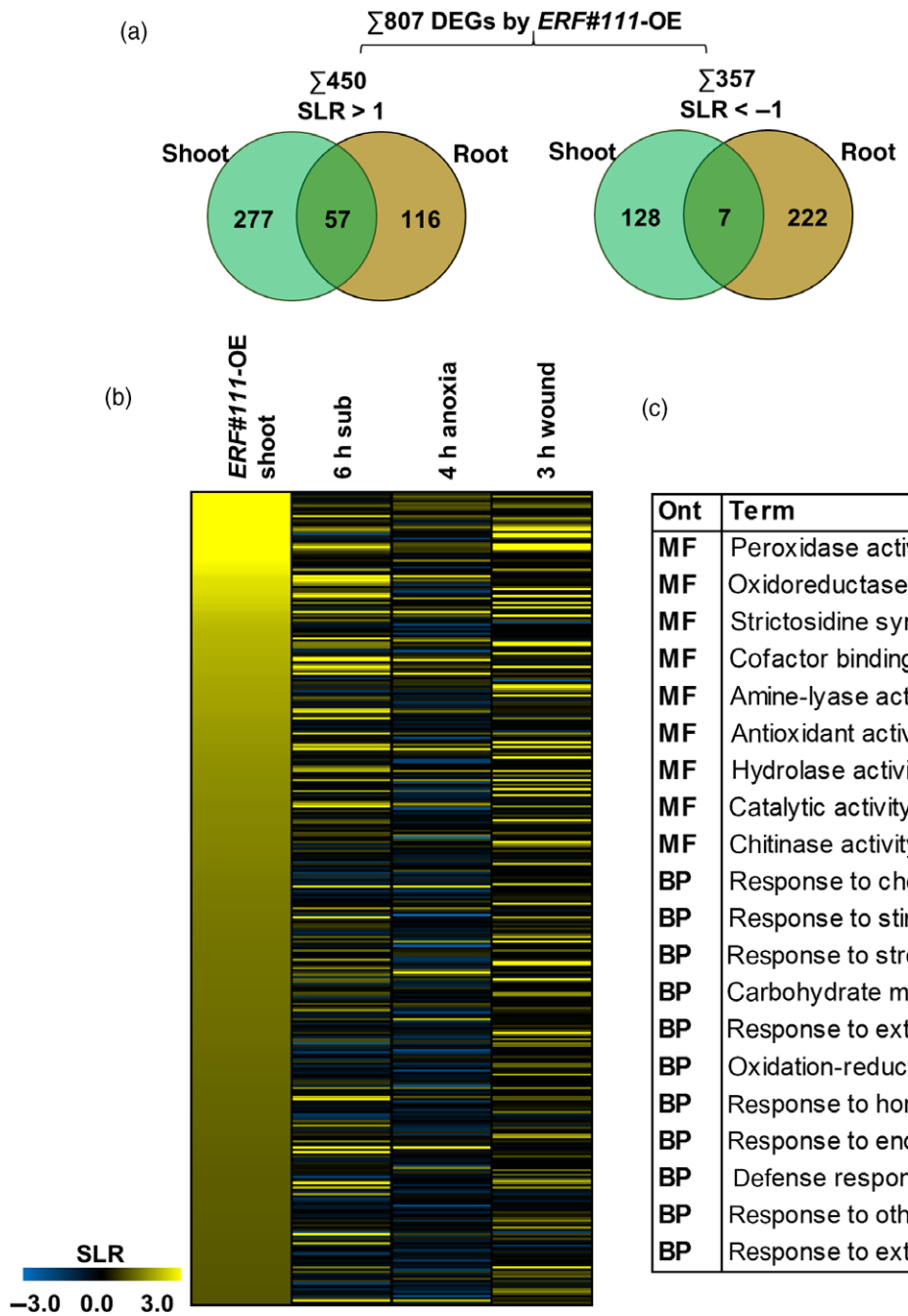

Ont	Term	*P*-value
MF	Peroxidase activity	1.4E-03
MF	Oxidoreductase activity	2.0E-03
MF	Strictosidine synthase activity	3.6E-03
MF	Cofactor binding	3.6E-03
MF	Amine-lyase activity	7.8E-03
MF	Antioxidant activity	9.2E-03
MF	Hydrolase activity	1.5E-02
MF	Catalytic activity	2.0E-02
MF	Chitinase activity	4.7E-02
BP	Response to chemical	8.3E-11
BP	Response to stimulus	1.6E-09
BP	Response to stress	9.0E-09
BP	Carbohydrate metabolic process	6.1E-05
BP	Response to external stimulus	5.4E-04
BP	Oxidation-reduction process	3.7E-03
BP	Response to hormone	8.5E-03
BP	Response to endogenous stimulus	1.2E-02
BP	Defense response	1.4E-02
BP	Response to other organism	2.0E-02
BP	Response to external biotic stimulus	2.1E-02

Figure 8. Gene expression profiling of *ERF#111*-OE plants. (a) Number of differentially expressed genes (DEGs) that were significantly upregulated (SLR > 1, $P < 0.01$) or downregulated (SLR < −1, $P < 0.01$) in shoots or roots of 7-day-old Arabidopsis *ERF#111*-OE lines. (b) Heatmap of shoot-specific DEGs caused by *ERF#111*-OE in comparison with microarray data from *Arabidopsis* seedlings that were submerged for 6 h in the dark (Hsu *et al.*, 2013), treated for 4 h with anoxia (Tsai *et al.*, 2014), and from leaves that were harvested 3 h after wounding (Wang *et al.*, 2015). Signal-Log2-Ratios are indicated by the intensity of the colour scale from −3 (blue) to 3 (yellow). (c) Selected Gene Ontology (GO) categories for molecular function (MF) and biological process (BP), significantly over-represented (*P*-values calculated by GOHyperGAll) in all DEGs that are upregulated (SLR > 1, $P < 0.01$) in the shoot by *ERF#111*-OE.

Identification of direct AtERF#111 target genes

As a next step, we aimed at identifying target genes that are likely to be regulated directly by the TF AtERF#111. We decided to compare gene expression after wounding between Col-0 and the *erf#111-2* mutant line by performing a microarray experiment, in which we wounded 3-week-old Arabidopsis leaves and harvested plant material 3 h after the treatment, similar to the experiment performed previously (Wang *et al.*, 2015). When comparing

the results of these wounding microarrays with our data, we could find a reasonable overlap: 448 out of 1415 DEGs from our wounding array were also modified in expression in the previous wounding array (Wang *et al.*, 2015). Interestingly, we could identify 328 genes that were significantly induced (SLR > 1, $P < 0.01$) upon wounding in the WT, but were not significantly changed in the *erf#111-2* mutant. One of these genes was of course *ERF#111* itself, confirming a true loss-of-function. However, changes in expression were not high enough to detect significant differences when comparing the samples from wounded WT and wounded *erf#111-2* mutant plants directly. This could either be due to the possibility that we had chosen an inadequate time point to identify differences between *erf#111-2* and WT, or and this seems more likely, that *AtERF#111* is not the only regulator of putative targets in response to wounding and that the effect might be covered by redundantly acting TFs.

To solve this problem, we chose another approach to identify direct AtERF#111 target genes by using a glucocorticoid-inducible protoplast assay. Technically, we expressed a translational fusion of AtERF#111 to a glucocorticoid receptor (ERF#111-HBD) in Arabidopsis protoplasts of the *erf#111-2* genotype. In this system, cytoplasmic-to-nuclear translocation of ERF#111-HBD is initiated by addition of the synthetic glucocorticoid dexamethasone (DEX) to the protoplast suspension. The effect of DEX treatment on target gene induction was measured in the presence or absence of the translation inhibitor cycloheximide (CHX), allowing for the distinction of direct and indirect target genes of AtERF#111. After 4 h of DEX treatment, protoplasts were harvested and RNA was isolated for subsequent microarray analysis. We identified 309 genes that are the sum of direct and indirect target genes (DEX treatment only) and 109 genes that were presumptive direct target genes (CHX + DEX treatment) (Figure 9 and Data S1). Among the direct target genes, all were significantly upregulated and none was significantly downregulated, supporting the conclusion that AtERF#111 is an activator of gene expression, and not a repressor as suggested by Pandey *et al.* (2005). By comparing the different microarray data, we could identify 15 direct target genes of AtERF#111, whose expression was also modified in response to wounding stress or in *ERF#111*-OE transgenic lines (Figures 8 and 9), again including the genes *SS3* and *TH8*, but also for example the *CYTOCHROME P450*, *CYP71B72* (*AT3G26200*). GO analysis of all identified direct AtERF#111 target genes revealed an enrichment of the biological processes response to external stimulus, defence response, response to wounding and response to other organism (Figure 9d), similar to the GO terms identified for the shoot-specific genes induced by stable overexpression of *AtERF#111*.

AtERF#111 transactivates selected target gene promoters

We used a protoplast transactivation system to study the transactivation potential of AtERF#111 on selected target promoters. To this end, an N-terminally HA-tagged AtERF#111 fusion (35S:HA-ERF#111) was cotransfected into Arabidopsis mesophyll protoplasts with the promoter of interest (a maximum of 2000 bp upstream of the start codon was used) fused to the firefly *Luciferase* gene (fLUC). Renilla *Luciferase* (rLUC) was used as an internal standard, and promoter activity was quantified by calculating fLUC activity relative to cotransfected rLUC activity (fLUC/rLUC). We chose the above-mentioned wounding and defence responsive genes *PDF1.2a*, *TH8*, *SS3* and *CYP71B22* as target promoter candidates (Figure 9e). Additionally, we also selected the hypoxia core gene *RHODANESE*, as well as the gene *EXPANSIN1* (*EXPA1*), which is thought to be involved in cell wall loosening and could explain the root hair phenotype of the *ERF#111*-OE lines. Except for *SS3*, we were able to detect significant transactivation of the selected target promoters of *PDF1.2a*, *TH8*, *CYP71B22, EXPA1* and *RHODANESE* by AtERF#111, demonstrating again that AtERF#111 positively regulates the transcriptional activity of these genes (Figure 10).

To further confirm the putative target genes of AtERF#111, we analyzed the expression of the selected genes in Col-0 and the *erf#111-2* loss-of-function line under control as well as under stress conditions (Figure 11). *RHODANESE* and *SS3* were induced upon wounding, but only a slightly lower expression was observed in *erf#111-2* compared to the WT (Figure 11c,d). *CYP71B22* showed no significant transcript changes 3 h after wounding stress in all genotypes (Figure 11e). To test the expression of the member of the plant defensins, we generated oligonucleotides amplifying *PDF1.1* to *PDF1.3* simultaneously, as their sequence is very similar. Interestingly, *PDF1.1-1.3* expression was significantly lower in the *erf#111-2* mutant in the control treatment compared with the WT, but the gene family was not induced by wounding under these experimental conditions (Figure 11a). The same could be observed for *EXPA1*, which also showed a lower expression in *erf#111-2* than in WT plants under control conditions, suggesting that AtERF#111 controls the expression of these two genes already under normal conditions.

One gene that was significantly less induced in response to wounding stress in *erf#111-2* than in the WT was *TH8* (Figure 11b). This trend was also observed in our microarray data: *TH8* was significantly induced in response to wounding in the WT, but not in *erf#111-2*. Nevertheless, the expression of *TH8* was not reduced to basal levels in the RT-qPCR experiment, again suggesting that AtERF#111 is not the only regulator of this gene.

As the expression of *RHODANESE* is strongly responsive to hypoxia, we also analyzed the transcript level after 4

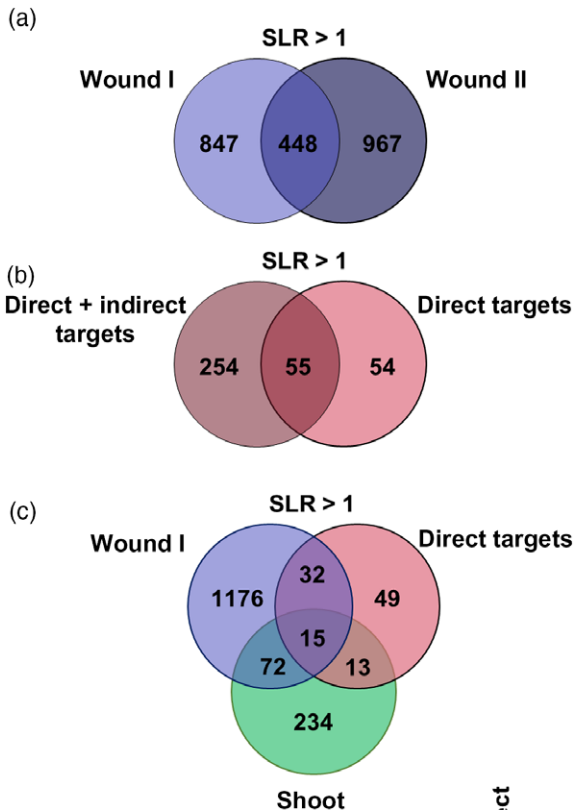

(d)

Ont	GO direct target genes	*P*-value
MF	Strictosidine synthase activity	1.3E-05
MF	Amine-lyase activity	2.9E-05
MF	Carbon-nitrogen lyase activity	2.8E-04
MF	Drug transmemb. transporter activity	7.2E-03
MF	Transmembrane transporter activity	7.4E-03
MF	Transporter activity	2.3E-02
MF	Iron-sulfur cluster binding	2.6E-02
MF	Metal cluster binding	2.6E-02
MF	O-methyltransferase activity	2.8E-02
BP	Response to external stimulus	6.4E-03
BP	Defense response	8.6E-03
BP	Response to w ounding	6.1E-03
BP	Defense response to other organism	1.9E-02
BP	Response to other organism	3.3E-03
BP	Response to external biotic stimulus	3.4E-03
BP	Response to biotic stimulus	4.9E-03
BP	Response to drug	3.3E-02
BP	Secondary metabolic process	3.0E-02
BP	Alkaloid metabolic process	4.1E-03
BP	Multi-organism process	1.5E-02
BP	Transmembrane transport	2.0E-03

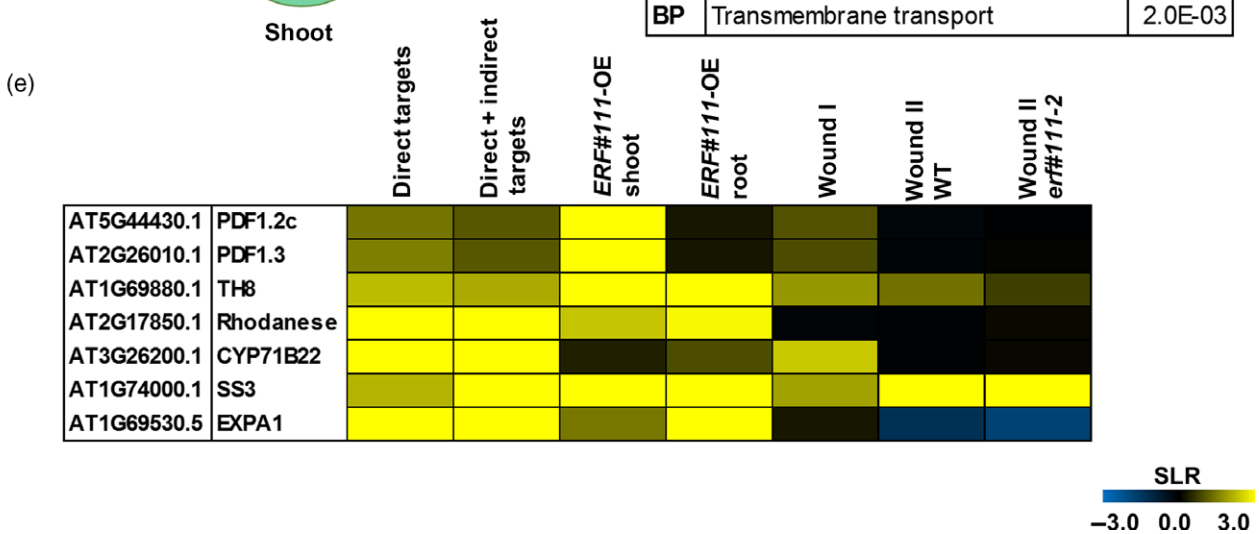

Figure 9. Identification of direct AtERF#111 target genes. (a) Number of DEGs (SLR > 1, $P < 0.01$) in the wounding microarray from Wang *et al.* (2015) (wound I) and our own wounding microarray (wound II). Plant material was in both cases collected 3 h after wounding of WT leaves. (b) Number of direct and direct + indirect AtERF#111 target genes identified by using the glucocorticoid-inducible protoplast assay. (c) Venn diagram showing overlapping DEGs between wound I, direct AtERF#111 target genes and genes induced by *ERF#111*-OE in the shoot. (d) Selected Gene Ontology (GO) categories for molecular function (MF) and biological process (BP), significantly overrepresented (*P*-values calculated by GOHyperGAll) in all direct target genes of AtERF#111. (e) Heatmap of selected genes comparing direct targets, direct + indirect targets, *AtERF#111*-OE in shoot and root as well as wound I and wound II (of WT and *erf#111-2* mutant plants). Signal-log2-ratios are indicated by the intensity of the colour scale from −3 (blue) to 3 (yellow).

and 8 h of hypoxia as well as 8 h hypoxia and 1 h re-aeration. Again, we could not detect any significant differences in expression between WT and *erf#111-2*, but we confirmed induction of this gene by hypoxia. These data suggest that AtERF#111 is not the only regulator of the wounding response. Indeed, several members of GXERFs in Arabidopsis are also strongly induced by wounding, among them ERF#108/RAP2.6, ERF#109/RRTF1, ERF#112, ERF#113/RAP2.6L, ERF#114, and ERF#115 (Figure S11, Ikeuchi *et al.*, 2017). Those TFs together with AtERF#111 might contribute to the transcriptional regulation of the wounding response.

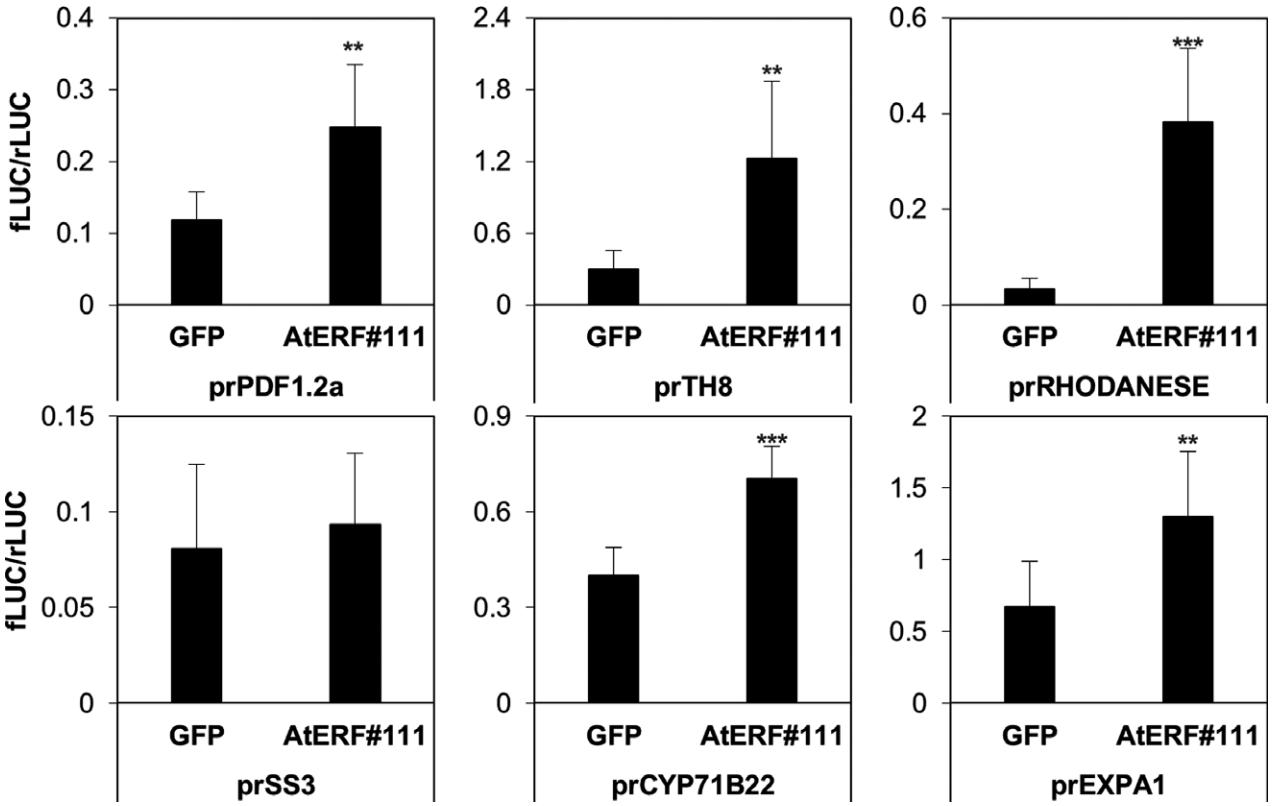

Figure 10. AtERF#111 transactivates selected target gene promoters. Luciferase (LUC) activity was measured in mesophyll protoplasts of the Arabidopsis mutant *erf#111-2* transiently expressing the effectors GFP (control) or AtERF#111 in combination with selected promotor constructs (e.g. prPDF1.2a, prTH8, prRHODANESE, prCYP71B22, prSS3, prGST6, and prEXPA1) fused to firefly *Luciferase* (fLUC). Promotor activity was quantified by monitoring fLUC activity relative to cotransfected renilla *Luciferase* (rLUC) and therefore has been calculated as fLUC/rLUC values. Data are means ± SD of six replicates. The asterisks indicate significant differences from controls at $***P < 0.001$ and $**P < 0.01$ (*T*-test).

DISCUSSION

AtERF#111 is a target of the ubiquitin/proteasome system

As mutants of the PRT6 N-degron pathway display a range of pleiotropic defects (Yoshida *et al.*, 2002; Graciet *et al.*, 2009; Holman *et al.*, 2009; Riber *et al.*, 2015; Gibbs *et al.*, 2016; Vicente *et al.*, 2017, 2018) and >200 proteins of the Arabidopsis genome start with an N-terminal Met−Cys, it is anticipated that there might be other MC-initiated targets of the PRT6 N-degron pathway, aside from the GVIIERFs. Among these, we investigated the function of the transcription factor AtERF#111, whose N-terminal region is highly conserved in protein homologues of other Brassicaceae species and initiates with MC (Figure S5). However, the analysis of the protein stability of (MC)/(MA)-ERF#111 constructs *in vivo* showed that both AtERF#111 versions were unstable and were degraded independently from their N-termini within 3 h (Figure 2b). Consequently, AtERF#111 does not represent a major target of the PRT6 N-degron pathway.

Not all proteins initiated with MC are true PRT6 N-degron pathway substrates, as N-degrons have to have several features. Aside from a primary destabilizing residue and an optimally positioned downstream lysine, the N-terminal region has to be unstructured to be accessible (Gibbs *et al.*, 2016; Dissmeyer *et al.*, 2018; Dissmeyer, 2019). One prominent example for a protein that evades the PRT6 N-degron pathway, despite containing the N-terminal motif, is SUB1-A1, which is a major determinant of submergence tolerance in rice (Fukao *et al.*, 2011; Gibbs *et al.*, 2011). For this protein, it was recently demonstrated that the C-terminus protects it from degradation (Lin *et al.*, 2019).

The half-life of the AtERF#111 protein might therefore be affected by other post-translational mechanisms, for example SUMOylation or ubiquitination on different target sites. Interestingly, AtERF#115, another member of the GXERFs, was tested to be a proteasome target (Heyman *et al.*, 2013), and an ubiquitination site was mapped to a lysine (K9) near the N-terminus (Walton *et al.*, 2016). An alignment of the GXERFs 8-15 revealed a conservation of this site in AtERF#111, AtERF#112, AtERF#114 and AtERF#115, suggesting that AtERF#111 might also be ubiquitinated at this position (Figure S6d). Indeed, we were able to show that the degradation of AtERF#111 is likely to be dependent on the ubiquitin/proteasome system, as an inhibition of

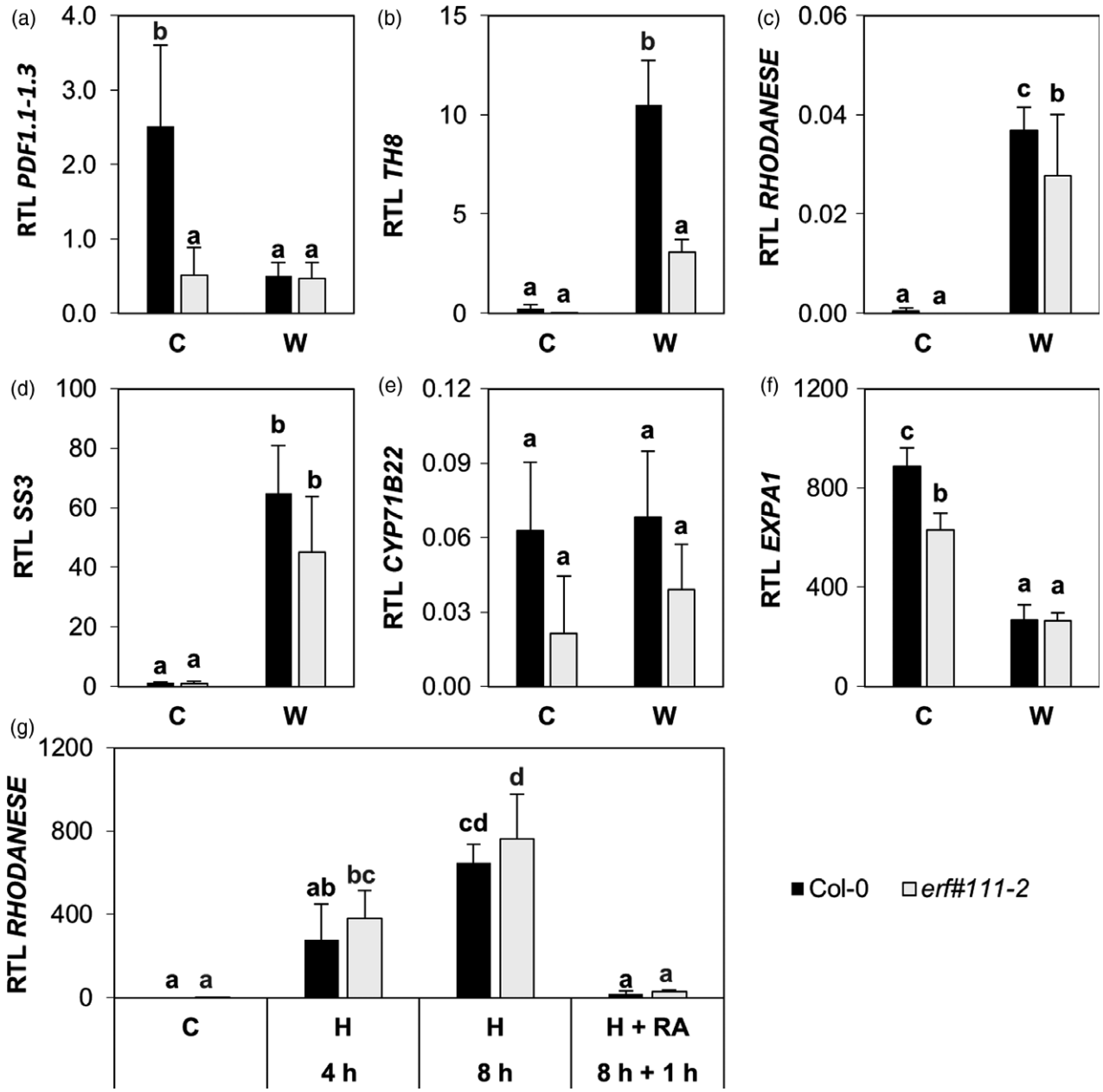

Figure 11. Analysis of AtERF#111 target gene expression in WT and *erf#111-2* after stress treatments. (a–f) RT-qPCR analyses of relative transcript levels (RTL) of *PDF1.1-1.3, TH8, RHODANESE, SS3, CYP71B22 and EXPA1* in leaves of 3-week-old WT Col-0 and *erf#111-2* mutant plants. Comparison of leaves from control plants (C) to 3 h wounded leaves (W). (g) RT-qPCR analysis of *RHODANESE* relative transcript levels (RTL) in 7-day-old seedlings that were treated with hypoxia (H) for 4 and 8 h as well as 8 h hypoxia followed by 1 or 16 h of re-aeration (RA). Controls (C) were kept under normoxic conditions. Transcript levels were normalized to *ELONGATION FACTOR 1A* (*EF1a*) mRNA. Values are means ± SD from three biological replicates (each with three technical replicates). Different letters indicate values that vary significantly at $P < 0.05$ (one-way ANOVA, Tukey HSD test).

the proteasome by MG132 resulted in a stabilization of the AtERF#111 protein (Figure 2c).

AtERF#111 is an activator of gene expression that is not related to ABA signalling or drought stress

In the context of this work, we examined the role of AtERF#111 in relation to ABA signalling and drought stress. AtERF#111, previously named ABA REPRESSOR 1 (ABR1) was described to be strongly induced upon exogenous ABA treatment, acting as an inhibitor of the ABA response (Pandey *et al.*, 2005). However, we were not able to confirm an involvement of AtERF#111 in ABA signalling. Essentially, we could not detect an induction of *AtERF#111* expression after treating Arabidopsis seedlings with

100 μM ABA (Figures 3c and 6). Song *et al*. (2016) monitored responses to ABA in the context of an RNA-seq time series experiment, including time points from 1 to 60 h after treating WT seedlings with 10 μM ABA in comparison with mock treatments. *AtERF#111* expression was not significantly modified at any tested time point. Furthermore, also microarray analysis of seedlings treated for 6 h with 10 μM ABA showed no *AtERF#111* induction (Liu *et al*., 2013).

In addition to an increase in *AtERF#111* transcript level upon ABA treatment, Pandey *et al*. (2005) observed a higher expression of selected ABA-marker genes in *erf#111* mutant lines in comparison with Col-0. In our experiment, the ABA-responsive genes *RAB18* and *RD22* did not show an altered expression between the *erf#111-2* mutant and the WT after ABA treatment, and also the OE lines displayed no downregulation of *RAB18* and *RD22* expression, as one would expect if AtERF#111 was an ABA repressor (Figure 3c). GO analysis of DEGs in the *ERF#111*-OE lines or of direct ERF#111 target genes did not include enriched GO categories related to ABA or drought (see Data S2). Additionally, no ABA- or drought-responsive genes, for example *RD29A*, *RD29B*, *RD22*, *RAB18*, *COR47*, or *DREB2A* were modified in expression in our microarray experiment of the *ERF#111*-OE lines (Data S1).

Furthermore, we also could not detect any differences between WT and *erf#111-2* in the germination assay on ABA-containing medium as well as in the root growth assay in the presence of ABA. In addition to Pandey *et al*. (2005), we included *ERF#111*-OE lines in our analysis, which showed no ABA insensitivity (Figure 3a,b, S6 and S7).

The synthesis of the phytohormone ABA is promoted by abiotic stresses that lead to a water deficit and osmotic stress, for example salt and low temperature, but mainly drought stress. Consequently, many genes induced by exogenous ABA treatment are also drought-induced (Finkelstein *et al*., 2002; Seki *et al*., 2002; Cutler *et al*., 2010; Sah *et al*., 2016). In addition to an induction of *AtERF#111* expression upon ABA treatment, Pandey *et al*. (2005) observed an increase in *AtERF#111* transcript level also upon drought stress. However, previously published data revealed contradicting results: a microarray experiment by Nishiyama *et al*. (2013) did not show an effect of drought stress on *AtERF#111* expression, whereas data by Ha *et al*. (2014) implied an induction of *AtERF#111* expression in response to drought. Drought stress treatments varied methodically in the corresponding experiments: Nishiyama *et al*. (2013) let plants progressively dry in pots by withholding water, whereas Ha *et al*. (2014) detached the aerial parts of the plants and exposed them to dehydration on paper. When we repeated the different drought treatments, we observed an induction of the drought-induced marker gene *RAB18* in both experiments, indicating that the plants are suffering from drought stress (Figure 4a). However, by letting plants dry in pots, we could not detect any changes in *AtERF#111* expression, confirming the findings of Nishiyama *et al*. (2013). We also let plants dry on paper similar to Ha *et al*. (2014), but instead of comparing changes in gene expression to intact plants in soil, we induced another control treatment, in which we covered the roots of the exposed plants with wet paper to avoid dehydration (Figure 6a). Thereby, we revealed that *AtERF#111* is strongly induced by mechanical stress, which occurs when the plant is removed from the soil and put on paper (Figure 4a). These findings highlight the importance of proper control treatments, which should be as similar to the actual stress treatment as possible. Therefore, the study from Ha *et al*. (2014) not only identified genes induced by drought treatment, but also those induced by mechanical stress, making a differentiation in this context impossible.

Apart from that, our experiments indicated that AtERF#111 is not a repressor, but an activator of gene expression, as all direct target genes of AtERF#111 identified by DEX-dependent nuclear localization of ERF#111 in the context of inhibited protein biosynthesis (Figure 9) were significantly upregulated and none was significantly downregulated in our microarray analysis. Furthermore, AtERF#111 was able to activate the promoters of the selected target genes (Figure 10). Taken together, our findings demonstrate that AtERF#111 is a transcriptional activator that seems to be neither involved in ABA signalling nor in the drought response.

AtERF#111 is involved in the wounding response

We were able to demonstrate that *AtERF#111* expression is strongly responsive to mechanical stress: its transcript level increased more than 300-fold within 1 h after wounding and decreased to basal levels after 6 h (Figure 4b). Furthermore, luminescence at wounded rosette leaves of stably transformed fLUC reporter lines expressing fLUC under the control of the promoter of AtERF#111 was evident (Figure 5). In line with this, we detected an induction of *AtERF#111* expression by H_2O_2 or MeJA, which are related to wounding stress (Figure 6). Additionally, the microarray analysis of *ERF#111-OE* plants showed a significant overlap of genes induced by *ERF#111*-OE in the shoot and by wounding (Figure 8b).

Also GO analysis of DEGs in *ERF#111*-OE transgenic plants highlighted responses to external stimuli, defence response or response to other organism (Figure 8c), supporting the hypothesis that AtERF#111 is involved in the wounding and defence response. We were able to identify a set of 109 genes that are directly regulated by AtERF#111 (Figure 9b). GO analysis of direct target genes included the GO-term 'response to wounding' (Figure 9d). By comparing the different microarray data, we could identify 15

direct target genes of AtERF#111, whose expression was also modified in response to wounding stress and by *ERF#111*-OE. In a protoplast transactivation assay, we showed that AtERF#111 activated the promoters of the selected target genes *PDF1.2a*, *TH8*, *RHODANESE*, *CYP71B22* and *EXPA1* (Figure 10).

When we compared gene expression after wounding between Col-0 and the *erf#111-2* mutant line by microarray analysis, we could not identify genes that were significantly lower expressed in *erf#111-2* in comparison with Col-0. Therefore, we hypothesized that AtERF#111 might not be the only regulator of putative targets in response to wounding. Additional RT-qPCR analysis of the selected target genes in Col-0 and *erf#111*-2 under control conditions and after wounding treatment showed that the only gene, which was significantly less induced in response to wounding stress in *erf#111-2* was *TH8* (Figure 11b), which is a *h*-type thioredoxin (TRX). In general, TRXs are small proteins that act as protein disulfide oxidoreductases and are involved in the regulation of the redox environment of the cell (Gelhaye *et al*., 2005). Arabidopsis TRXs are organized in at least five different families (*f*, *m*, *x*, *o* and *h*), whereas group *h* contains eight genes that are thought to encode for cytosolic proteins in Arabidopsis (Meyer *et al*., 2002; Reichheld *et al*., 2002). For one member of this group, *AtTRXh5*, an upregulation during wounding, abscission and senescence as well as during contact with the bacterial pathogen *Pseudomonas syringae* was shown (Laloi *et al*., 2004). Additionally, AtTRXh5 is required for the response to victorin, a phytotoxin which induces programmed cell death in sensitive plants (Sweat and Wolpert, 2007; Lorang *et al*., 2012). Only very little information is available on TH8, but we observed a clear induction upon wounding and showed that it is a direct target gene of AtERF#111 (Figures 9e, 10 and 11). The expression of *TH8* was not reduced to basal levels after wounding in the *erf#111-2* mutant in comparison with the WT, suggesting again that the loss of AtERF#111 is covered by redundantly acting TFs.

Indeed, several of the eight members of GXERFs in Arabidopsis are also strongly induced by wounding, among these ERF#108/RAP2.6, ERF#109/RRTF1, ERF#112, ERF#113/RAP2.6L, ERF#114 and ERF#115 (Figure S11, Ikeuchi *et al*., 2017). Just recently, the hypothesis was published that members of the GXERF TFs coordinate stress signalling with the activation of wound repair mechanisms (Heyman *et al*., 2018). With the exception of ERF#112, they share a subfamily-specific conserved motif near the N-terminus (Figure S5d). This was shown, at least for ERF#114 and #115, to be important for the heterodimerization with TFs of the GRAS domain type – an interaction that turns these GXERFs into highly potent cell division activators (Heyman *et al*., 2016, 2018).

Interestingly, the expression of another member of the GXERFs, *AtERF#109* – named *REDOX RESPONSIVE TRANSCRIPTION FACTOR1* (*RRTF1*) – is mediated by the WRKY TFs 18, 40, and 60, and is aside from wounding highly responsive to JA and reactive oxygen species (ROS), whereas the gene product itself enhances ROS production (Wang *et al*., 2008; Pandey *et al*., 2010; Matsuo *et al*., 2015). In the context of a genome-wide binding study, Birkenbihl *et al*. (2017) showed that *AtERF#111* is also a target of the WRKY TFs 18, 33 and 40, which modulate pathogen-triggered immune responses in plants. This dataset included the information that *ERF#111*, *#112*, and *#115* are targets of WRKY18, 33 and 40, and confirmed *ERF#109* being a target of WRKY18 and 40. It was hypothesized that ERF#109 is important for controlling the balance of ROS within the cell (Matsuo *et al*., 2015). *ERF#109*-OE plants displayed enhanced susceptibility to the plant pathogen *Alternaria brassicae*, which could be weakened by applying antioxidants or free radical scavengers (Matsuo *et al*., 2015). In addition, *rrtf1* mutants did not show an obvious phenotype, whereas OE of *ERF#109* led to the production of more and longer root hairs (Cai *et al*., 2014). Correspondingly, we observed that overexpression of *AtERF#111* also significantly increased elongation and production of root hairs in comparison with Col-0 (Figure 7). Microtome sections of *ERF#111*-OE lines showed root hairs that were not only produced in root hair cells, but also in the non-hair cells that normally lack root hairs (Figure 7e). The phenomenon of the ectopic development of root hairs in the non-hair positions has been shown to be caused by abiotic stresses, such as phosphorus or iron starvation (Müller and Schmidt, 2004).

One candidate gene that might be responsible for the observed root hair phenotype of *AtERF#111-OE* plants is *EXPA1*, as we noticed no further root hair- or root epidermis-specific genes modified in expression (Data S1), and *EXPA1* is also a direct target gene of ERF#111 (Figure 9e). Expansins are proteins without hydrolytic activity that participate in cell wall loosening (Cosgrove, 2000; Choi *et al*., 2006). *AtEXPA7*, another member of α expansins in Arabidopsis, was shown to influence root hair initiation and root growth (Cho and Cosgrove, 2002). *EXPA1* was reported to be induced by cytokinin in the root, which is involved in controlling cell differentiation initiation (Bhargava *et al*., 2013; Pacifici *et al*., 2015). Interestingly, the development of root hairs was delayed in the *expa1* mutant, indicating a setback in cell differentiation (Pacifici *et al*., 2018). These data support the hypothesis that EXPA1 could be connected to the root hair phenotype of AtERF#111-OE plants. Notably, the fact that the expression of other genes related to root cell differentiation was unchanged in the *AtERF#111-OE* genetic background hints towards a function of *AtERF#111* in stress responsive

modulation of root morphology, rather than developmental hair cell specification.

Is the induction of *AtERF#111* related to mechanical stress during submergence?

We showed that the expression of *AtERF#111* is induced upon hypoxia and submergence (Figure 1a,b). Datasets of RNA- as well as ribosome sequencing confirmed its induction upon submergence, which is shoot-specific (van Veen *et al.*, 2016; Yeung *et al.*, 2018). *AtERF#111* seems to be not a target of the GVIIERFs, as its promoter sequence does not contain any HRPE and we could not detect differences in *AtERF#111* expression in Col-0 and the PRT6 N-degron pathway mutant *prt6-1* (Figure S2). In line with the assumption that various members of the GXERFs might act redundantly, we could not observe any variation in submergence survival of Col-0 and *erf#111-2* (Figure 1c). Indeed, also other GXERFs show enhanced expression under submergence, for example *ERF#108*, *ERF#112*, *ERF#113* and *ERF#114* (Lee *et al.*, 2011; Hsu *et al.*, 2013; Yeung *et al.*, 2018) and/or re-aeration after hypoxic treatment, for example *ERF#108*, *ERF#109*, *ERF#113* and *ERF#114* (Branco-Price *et al.*, 2008; Tsai *et al.*, 2014).

Additionally, AtERF#111 seems to be no major regulator of the anaerobic response. Only one of the 49 core HRGs (Mustroph *et al.*, 2009), *RHODANESE*, was upregulated by *ERF#111*-OE in roots and shoots and was identified to be directly regulated by AtERF#111 (Figure S10a, 9e and 11e). Expression analysis of *RHODANESE* revealed no differences in response to hypoxia between Col-0 and *erf#111-2* (Figure 11c).

When comparing all DEGs caused by *ERF#111*-OE to submergence microarray data (Hsu *et al.*, 2013), we found a significant overlap between the data sets (Figures 8b and S10b). Submergence is a compound stress, including not only low-oxygen availability, but also low light, nutrient deficiency, high risk of infection or mechanical stress, and therefore many genes are modified in expression. Interestingly, innate immunity marker genes as well as members of the WRKY TF family are strongly induced during submergence (Hsu *et al.*, 2013). Among these, WRKY22 was shown to activate the immune response, thereby increasing the resistance towards the pathogen *Pseudomonas syringae* (Hsu *et al.*, 2013). This is a good example how submergence can stimulate the immune response of the plant, as the risk of wounding or pathogen infection increases after flooding.

Aside from *WRKY22*, also *WRKY18*, *WRKY33*, and *WRKY40* are significantly induced upon submergence (Hsu *et al.*, 2013), and all three are also upregulated by anoxia (Tsai *et al.*, 2014) and wounding stress (Wang *et al.*, 2015). As *AtERF#111* was shown to be regulated by WRKY18, 33 and 40 as mentioned above (Birkenbihl *et al.*, 2017), we speculated that the regulation of *AtERF#111* expression might be related to mechanical stress during submergence. As *AtERF#111* is not only induced by submergence, but also by hypoxia, one could also imagine that submerged plants might expect to be mechanically stressed or wounded when the flood recedes, as the hypoxia treatment simulates the low-oxygen availability during submergence.

CONCLUSION

In the present study, we identified AtERF#111 as a wounding-responsive TF, whose expression is also induced upon hypoxia and submergence. We could neither confirm AtERF#111 acting as a repressor of ABA signalling, nor an involvement in the drought response. Despite its N-terminal MC motif, this potential substrate could not be shown to be a target of the PRT6 N-degron pathway. By replacing the conserved Cys2 residue with Ala and comparing protein abundance, both (MC) and (MA)AtERF#111 demonstrated instability, whose degradation is yet dependent on the ubquitin/proteasome system. By microarray analyses, we could define a set of genes that show a link to wounding stress and are directly regulated by AtERF#111, thereby acting as a transcriptional activator of gene expression. However, resolving the function of AtERF#111 in combining the responses to submergence and wounding remains a future challenge. The likely redundancy of AtERF#111 and other GXERFs in coordinating stress singaling makes it necessary to generate higher order mutants to further investigate their function.

EXPERIMENTAL PROCEDURES

Plant material and growth conditions

Arabidopsis (*Arabidopsis thaliana*) ecotype Columbia (Col-0) was used as the WT. Seeds of the T-DNA insertion lines SALK_094151C (*erf#111-1*) and SALK_012151C (*erf#111-2*) were ordered from the Nottingham Arabidopsis Stock Centre, *prt6-1* (SAIL_1278_H11) was obtained from Julia Bailey-Serres. Seeds of the quadruple mutant *pyr1 pyl1 pyl2 pyl4* were obtained from Sean Cutler (Park *et al.*, 2009). Seeds were surface-sterilized and sown on Murashige and Skoog (MS) medium (Duchefa, Haarlem, The Netherlands, including 1% (w/v) sucrose, 1% (w/v) agar), stratified (3 days darkness, 4°C) and grown for the indicated time periods in phytocabinets under long-day (LD) conditions (23°C, 16 h/8 h light/dark cycle; 100 μmol of photons m^{-2} sec^{-1}). For experiments with adult plants, 7-day-old seedlings were planted into soil (soil:vermiculite, 2:1; for submergence experiments one-part sand was added to two-parts of the soil mixture) and grown for 2–3 weeks under short-day (SD) conditions (23°C, 8 h/16 h light/dark cycle; 100 μmol of photons m^{-2} sec^{-1}). For protoplast experiments, seeds were directly sown on soil and plants were grown for 4 weeks under SD conditions.

Hypoxia treatments and submergence experiments

For hypoxia treatments, 7-day-old seedlings grown on MS medium were used. 2 h after the onset of the photoperiod, open Petri dishes were placed into a desiccator for the indicated time periods

and constantly flushed with 100% nitrogen under LD conditions in the light. For re-aeration treatments, the Petri dishes were removed from the desiccator and placed under LD conditions in air. Controls were also kept under ambient LD conditions in air for the same time periods.

For submergence experiments followed by RT-qPCR analysis, Arabidopsis plants were grown until the 10-leaf stage under SD conditions. Two hours after the beginning of the photoperiod, plants were either kept under control conditions air + light (AL) or were transferred to air + darkness (AD) or to submergence + darkness (SD). After 24 h, leaf material (except cotyledons) was harvested (two plants were pooled per treatment). For submergence survival experiments, plants were submerged in plastic tubs with temperature adjusted water in darkness for 4, 5, 6 and 7 days, whereas control plants were kept in dark and air for the same time (10 plants per treatment). After 2 weeks of recovery under SD conditions, pictures were taken and the survival rate of the plants was scored, which was determined as the ability to form new leaves. After all treatments, plant material was immediately frozen in liquid nitrogen and stored at −80°C until further processing.

ABA experiments

For the germination assay in the presence of ABA, seeds of the same age of WT, *erf#111-2*, *ERF#111*-OEI and OEII, *prt6-1* and *pyr1 pyl1 pyl2 pyl4* were placed on MS agar plates (for all ABA experiments described here, MS medium was used without sucrose) with 0, 0.3, 0.5 and 0.7 μM ABA (Duchefa, A0941.0100). The ability to establish germination was documented after 10 days (16 h photoperiod). For the expression analysis of ABA-responsive genes, 7-day-old seedlings were sprayed with 100 μM ABA (solvent ethanol) for 4 h and control plants were equally treated with a mock solution. For the root growth assay, seedlings were grown for 3 days on MS agar plates and then transferred on MS agar plates supplied with 0, 5, 10, 30, 50 or 100 μM ABA. The root lengths were measured after an additional 14 days ($n > 10$ per replicate and treatment).

Wounding and drought treatments

For the wounding experiments, all rosette leaves of 3-week-old plants grown on soil (eight leaf stage, 8 h photoperiod) were gently wounded with a needle, whereas non-wounded control plants were kept in parallel. Leaf material (except cotyledons; two plants were pooled per treatment) was harvested after the indicated time points. For the progressive drought treatments in pots, 3-week-old plants grown on soil were exposed to drought stress (D) by letting them grow for 9 days without watering, whereas controls (C) were well watered (=C/D pot). For drought treatment on paper, the whole plants were removed from the soil and exposed to dehydration on papers for 3 h, whereas the roots of the exposed control plants were covered with wet paper (=C/D paper).

In vivo bioluminescence imaging

For the imaging of fLUC activity, the leaves of intact plants of Col-0 and plants expressing prAtERF#111:fLUC (T1 generation) were cut with scissors. After an incubation time of 90 min, the rosettes of the plants were evenly sprayed with 2 mM D-luciferin (PJK, Kleinblittersdorf, Germany) + 0.1% (v/v) Triton X-100. Pictures of bioluminescence were taken in a low-light imaging system (Intas) with a camera shutter time of 20 min.

H_2O_2, MeJA and ACC treatment

Seven-day-old WT seedlings grown on MS agar plates were sprayed with 10 mM H_2O_2, 50 μM MeJA (Sigma-Aldrich, Taufkirchen, Germany, 392707) or 500 μM ACC (Sigma-Aldrich, Taufkirchen, Germany, A3903). Control plates were equally treated with the according solvents (e.g., ethanol or water). For each treatment 0.01% Tween-20 was added and plant material was harvested after 1 h.

Microtome sections and analysis of the root hair phenotype

For microtome sections, 7-day-old roots of Col-0 and *erf#111*-OEI and OEII were used. For chemical fixation, roots were vacuum infiltrated for 30 min with fixation solution (2% (w/v) paraformaldehyde, 1% (v/v) glutaraldehyde, 1% (w/v) caffeine, 0.01% Triton X-100 in 0.1 M phosphate buffer (pH 7.0)) and incubated overnight at 4°C. For subsequent mechanical fixation, the roots were washed two times with 0.1 M phosphate buffer (pH 7.4) and dehydrated in baths of 50, 70, 90, 95 and 100% ethanol, 1-butanol/ethanol 1:1 (v/v), and 100 % 1-butanol, for 30 min each. For embedding, the *Technovit 7100* plastic embedding system (Kulzer Technique, Wehrheim, Germany) was used according to manufacturer's instructions. Root sections (15 μm) were made using the 2050 SuperCut Microtome (Leica Microsystems, Wetzlar, Germany) and viewed under a DM1000 microscope (Leica Microsystems).

To calculate the length ($n > 130$) and number ($n > 14$) of root hairs at the root tip as well as at the root base, photographs of 7-day-old seedlings were taken with a RS Photometrics CoolSnap camera coupled to a M3B stereomicroscope (Wild Heerbrugg, Heerbrugg, Switzerland). Root lengths were measured using the ImageJ software (version 1.44p; https://imagej.nih.gov/ij/).

RNA isolation and PCR analysis

RNA isolation, cDNA synthesis, reverse transcription standard and quantitative PCR (RT-qPCR) were performed as described previously (Klecker *et al.*, 2014). RT-qPCR was performed using the iQ SYBR Green Super mix and the CFX Connect Real-Time PCR Detection System (Bio-Rad, Feldkirchen, Germany). All primers are listed in Data S3. Three biological replicates, each with three technical repetitions, were measured. Relative expression values were determined by the $2^{-\Delta CT}$ method and normalized to *ELONGATION FACTOR 1A* (*EF1a*).

Plant transformation and confocal imaging

To generate stable Arabidopsis lines as well as transiently transformed tobacco, binary expression vectors were transformed into *Agrobacterium tumefaciens*, strain GV3101 (Koncz *et al.*, 1984). Tobacco leaves were transiently transformed with the *Agrobacterium* solution as described by Bendahmane *et al.* (2000) and after 3 days, leaf discs were collected for confocal imaging. For generation of stable overexpression lines, Arabidopsis plants were transformed by floral dip as described previously (Clough and Bent, 1998). After 4 weeks, the seeds were harvested and positive transformants were identified by antibiotic resistance (Kanamycin). Homozygous transgenic plants were obtained in the T3 generation.

For subcellular localization and imaging of transiently transformed tobacco, GFP fluorescence was analyzed by confocal laser scanning microscopy using LEICA TCS SP2 (Leica Microsystems, at λ_{ex} 488 nm for GFP and chlorophyll excitation, λ_{em} 530–555 nm for GFP and 650–720 nm for chlorophyll emission).

Vector construction and plasmid purification

The N-terminal HA-tagged effector construct used for protoplast transfection p35S:HA-GFP has been described before (Klecker

et al., 2014) and p35S:HA-AtERF#111 was constructed by recombining the coding sequence of AtERF#111 into the Gateway vector p35S:HA-GW (Ehlert *et al.*, 2006). For the firefly *Luciferase* reporter constructs prPDF1.2a:fLUC, prTH8:fLUC, prRHODANESE:fLUC, prSS3:fLUC, prCYP71B22:fLUC, and prEXPA1:fLUC, the 5′ upstream sequences (a maximum of 2000 bp) from the start codon were amplified from Col-0 genomic DNA with specific primer pairs (Data S3). PCR products as well as the vector pBT10GA-L4UAS (Wehner *et al.*, 2011) were digested with *Nco*I and *Bam*HI before ligation, removing the GAL4UAS sequence. For the normalization of gene expression, the p35S promotor and the coding sequence of renilla *Luciferase* was isolated from p70SRUC (Stahl *et al.*, 2004) and integrated into pBT10GAL4UAS, thereby removing the GAL4UAS sequence and the firefly coding sequence and generating the new construct pBT10-rLUC.

For the construction of (MA)AtERF#111 and (MC)AtERF#111, the *AtERF#111* coding sequence was amplified with a forward primer that introduced a mutation in the second codon, thereby replacing the N-terminal Cys2 with Ala to inhibit a potential degradation by the Cys branch of the PRT6 N-degron pathway. For C-terminal translational fusions, the reverse primer was designed without the stop codon. Products were recombined into the Gateway entry vector pDONR221 using BP clonase (Invitrogen, Karlsruhe, Germany). Entry clones were then recombined into different Gateway destination vectors using LR clonase (Invitrogen). For *Agrobacterium*-mediated plant transformation, the destination vectors pMDC83-GFP (Curtis and Grossniklaus, 2003) and p35S:HF-GATA (Mustroph *et al.*, 2010) were used.

To generate fLUC reporters for stable plant genome integration, the promoter region of AtERF#111 (1302 bp) was amplified from Col-0 gDNA with specific Gateway recombination-compatible primers (Data S3). Products were first recombined into the Gateway entry vector pDONR201 and then recombined into the Gateway destination vector pBGWL7 (Karimi *et al.*, 2005).

For the glucocorticoid-inducible protoplast assay, entry clones (GFP was used as a control) were recombined into p35S:rfA-HBD (a kind gift from Monika Tomar). For protein stability analysis in protoplasts, (MC)AtERF#111 and (MA)AtERF#111 were recombined in the destination vector p35S:GW-HA to gain a C-terminal HA-tag. Plasmids were purified using the NucleoBond PC 500 Midi Kit (Macherey-Nagel, Düren, Germany) and stored at −20°C until use.

Protoplast isolation, transient transformation and treatment

Protoplast isolation and transient transformation followed by luciferase activity measurements were performed as described previously (Klecker *et al.*, 2014). For each transformation, a concentration of approximately 3.5×10^5 Arabidopsis mesophyll protoplasts per ml was used. For promoter transactivation assays, 200 μl of protoplast solution was transformed with 4 μg of the reporter plasmid, 2 μg of the effector plasmid and 0.5 μg of the normalization vector pBT10-rLUC. For measurements, 20 microliters of protoplast solution was mixed with 50 μl of the respective substrate solution. Light emission was measured with the GloMax 96 Microplate Luminometer (Promega, Mannheim, Germany) with an integration time of 3 sec. For the glucocorticoid-inducible protoplast assay followed by microarray analysis, 400 μl of protoplast solution was transformed with 20 μg of *35S:AtERF#111*-HBD or *35S:GFP*-HBD, incubated over night for 18 h under LD conditions and then mixed with 50 μM CHX (Sigma-Aldrich, C7698), or the same amount of the solvent dimethyl sulfoxide (DMSO). After 30 min incubation with CHX, 10 μM DEX (Sigma-Aldrich, D4902) was added to the suspension and incubated for additional 4 h under LD conditions. Afterwards, cells were frozen in liquid nitrogen and RNA was isolated.

For protein stability assays by western blot analysis, protoplasts were transformed according to Wu *et al.* (2009). Here, 30 μg of plasmid DNA (effector plasmids encoding 35S:(MC)AtERF#111-HA or 35S:(MA)AtERF#111-HA, see above) were transformed in 600 μl reaction volumes containing each ~$16.5*10^6$ cells. After overnight expression, protoplast suspensions were split into 180 μl of samples and supplemented with 50 μM MG132 (UBP Bio, Aurora, CO, USA, F1101) or a DMSO mock control. For the 3 h chases, 100 μM CHX (Santa Cruz Biotechnology, Heidelberg, Germany, sc-3508) were added immediately after addition of proteasome inhibitor. For 1 h chases, samples were treated 2 h later and all samples were harvested after 1 h additionally by centrifugation (200 ***g***, 1 min). Pellets were frozen in liquid nitrogen. For SDS-PAGE analysis, pellets were resuspended in 116 μl of extraction buffer (50 mM Tris−HCl, pH 7.6; 150 mM NaCl; 20 mM NaF; 1% (v/v) Nonidet P-40; 0.5% (w/v) deoxycholate; 10 mM $Na_4P_2O_7$; 1 mM EDTA; 0.5 mM EGTA; 1 mM DTT; 1× cOmplete EDTA-free Protease Inhibitor Cocktail (Roche, Mannheim, Germany)), and incubated for 15 min at 68°C with 3× SDS sample buffer. Protein was detected using anti-HA antibody (Covance HA.11, MMS-101R; 1:1000 diluted in TBST (50 mM Tris−HCl, pH 8; 150 mM NaCl; 0.1% Tween-20) containing 3% skimmed milk powder (Roth, Karsruhe, Germany, T145.3)) as primary antibody in combination with HRP-coupled anti-mouse secondary antibody (Pierce, 31437; 1:5000 diluted in the same blocking buffer as above).

Microarray analysis

For microarray experiments, total RNA was isolated using the RNeasy Plant Mini Kit (Qiagen, Hilden, Germany). For analysis of the effect of *ERF#111* overexpression, we extracted RNA from 7-day-old seedlings from two independent OE lines, *ERF#111*-OEI and *ERF#111*-OEII, which were separated in roots and shoots, and compared the expression with that of roots and shoots of Col-0. For the wounding microarray, RNA was extracted from whole rosettes (except cotyledons) of 3-week-old Col-0 and *erf#111-2* mutant plants 3 h after wounding. For the glucocorticoid-inducible protoplast assay, RNA was extracted from p35S:AtERF#111-HBD and 35S:GFP-HBD transformed protoplasts isolated from *erf#111-2* mutant plants.

The RNAs were processed by the Genomics and Bioinformatics core facility (University of Bayreuth). For hybridization of the probes, the Arabidopsis 4×44k array from Agilent Technologies was used (design ID 021169). Here, 150 ng of total RNA of each sample were labelled using the Low Input Quick Amp Labelling Kit as recommended by the manufacturer (manual G4140-90050, Agilent Technologies). Dye-swap experiments were included in the microarray design. The hybridization experiments were performed as recommended in the Two-Colour Microarray-Based Gene Expression Analysis protocol (manual G4140-90050, Agilent Technologies). Processed microarrays were scanned using a high-resolution microarray scanner (Agilent Technologies) and spot intensities were quantified using Agilent's feature extraction software.

Data were analyzed with the LIMMA package using the program R. Every array was background corrected and normalized with the Loess-algorithm, between the arrays the Quantile method was used for normalization. Significantly modified genes with a difference in expression greater than 2 (Signal-Log2-Ratio >1) and a *P*-value < 0.01 were chosen for further analysis. For comparison of our microarray data to already published microarray experiments,

the data were downloaded from the GEO database and reanalyzed.

Gene ontology analysis

The lists of DEGs identified by microarray analysis were evaluated for an enrichment of the GO categories specific biological process, molecular function or cellular compartment by using the GOHyperGAll function in the program R (Horan *et al.*, 2008). GO categories with an adjusted $P < 0.05$ were classified as significantly enriched.

ACCESSION NUMBERS

Raw data have been deposited at the GEO database under accession number GSE121587. AGI codes for Arabidopsis genes studied are available in Data S3.

ACKNOWLEDGEMENTS

We thank Pia Schuster, Michaela Hochholzer and Andrea Kirpal for excellent technical assistance. This work was supported by the 'Stifterverband für die Deutsche Wissenschaft' (H140 5409 9999 15625) to AM, by the DFG (German Research Foundation) to AM (MU 2755/4-1) and ND (DI 1794/3-1), by the ScienceCampus Halle, Plant-Based Bioeconomy, and the Leibniz Institute of Plant Biochemistry (IPB).

AUTHOR CONTRIBUTIONS

JB, ND, MK, ARW, and AM planned and designed the experiments. JB, WR, MK, LM, and ARW performed experiments. JB and AM analyzed the data and wrote the manuscript. All authors read and commented on the manuscript.

CONFLICT OF INTEREST

The authors have no conflict of interest to declare.

SUPPORTING INFORMATION

Additional Supporting Information may be found in the online version of this article.

Figure S1. Response to flooding stress in different Arabidopsis accessions.

Figure S2. Expression analysis of *AtERF#111* upon hypoxia.

Figure S3. Analysis of *AtERF#111* T-DNA insertion alleles.

Figure S4. Survival after submergence of *erf#111-2* and *ERF#111*-OEII in comparison with Col-0.

Figure S5. Protein multiple sequence alignments of AtERF#111.

Figure S6. Germination assay in the presence of ABA.

Figure S7. Evaluation of root growth and seedling weight in the presence of ABA.

Figure S8. Representative pictures of the drought/wounding treatments.

Figure S9. The expression of *AtERF#111* is induced by mechanical stress.

Figure S10. Venn diagrams showing overlapping DEGs.

Figure S11. Expression of other GXERFs upon wounding.

Data S1. Microarray data presented in this publication.

Data S2. GO analysis of differentially expressed genes.

Data S3. Material used in this publication.

Data S4. References.

REFERENCES

Alfieri, L., Bisselink, B., Dottori, F., Naumann, G., de Roo, A., Salamon, P., Wyser, K. and Feyen, L. (2017) Global projections of river flood risk in a warmer world. *Earths Future*, **5**, 171–182.

Bailey-Serres, J. and Voesenek, L.A.C.J. (2008) Flooding stress: acclimations and genetic diversity. *Annu. Rev. Plant Biol.* **59**, 313–339.

Bailey-Serres, J., Fukao, T., Gibbs, D.J., Holdsworth, M.J., Lee, S.C., Licausi, F., Perata, P., Voesenek, L.A.C.J. and van Dongen, J.T. (2012) Making sense of low oxygen sensing. *Trends Plant Sci.* **17**, 129–138.

Bhargava, A., Clabaugh, I., To, J.P., Maxwell, B.B., Chiang, Y.-H., Schaller, G.E., Loraine, A. and Kieber, J.J. (2013) Identification of cytokinin-responsive genes using microarray meta-analysis and RNA-Seq in Arabidopsis. *Plant Physiol.* **162**, 272–294.

Birkenbihl, R.P., Kracher, B. and Somssich, I.E. (2017) Induced genome-wide binding of three Arabidopsis WRKY transcription factors during early MAMP-triggered immunity. *Plant Cell*, **29**, 20–38.

Branco-Price, C., Kaiser, K.A., Jang, C.J.H., Larive, C.K. and Bailey-Serres, J. (2008) Selective mRNA translation coordinates energetic and metabolic adjustments to cellular oxygen deprivation and reoxygenation in *Arabidopsis thaliana*. *Plant J.* **56**, 743–755.

Bui, L.T., Giuntoli, B., Kosmacz, M., Parlanti, S. and Licausi, F. (2015) Constitutively expressed ERF-VII transcription factors redundantly activate the core anaerobic response in *Arabidopsis thaliana*. *Plant Sci.* **236**, 37–43.

Cai, X.-T., Xu, P., Zhao, P.-X., Liu, R., Yu, L.-H. and Xiang, C.-B. (2014) Arabidopsis ERF109 mediates cross-talk between jasmonic acid and auxin biosynthesis during lateral root formation. *Nat. Commun.* **5**, 5833.

Cho, H.-T. and Cosgrove, D.J. (2002) Regulation of root hair initiation and expansin gene expression in Arabidopsis. *Plant Cell*, **14**, 3237–3253.

Choi, D., Cho, H.-T. and Lee, Y. (2006) Expansins: expanding importance in plant growth and development. *Physiol. Plant.* **126**, 511–518.

Choy, M.-K., Sullivan, J.A., Theobald, J.C., Davies, W.J. and Gray, J.C. (2008) An Arabidopsis mutant able to green after extended dark periods shows decreased transcripts of seed protein genes and altered sensitivity to abscisic acid. *J. Exp. Bot.* **59**, 3869–3884.

Clough, S.J. and Bent, A.F. (1998) Floral dip: a simplified method for *Agrobacterium*-mediated transformation of *Arabidopsis thaliana*. *Plant J.* **16**, 735–743.

Cosgrove, D.J. (2000) Loosening of plant cell walls by expansins. *Nature*, **407**, 321–326.

Curtis, M.D. and Grossniklaus, U. (2003) A Gateway cloning vector set for high-throughput functional analysis of genes in planta. *Plant Physiol.* **133**, 462–469.

Cutler, S.R., Rodriguez, P.L., Finkelstein, R.R. and Abrams, S.R. (2010) Abscisic acid: emergence of a core signaling network. *Annu. Rev. Plant Biol.* **61**, 651–679.

Dissmeyer, N. (2019) Conditional protein function via N-degron pathway-mediated proteostasis in stress physiology. *Annu. Rev. Plant Biol.* **70**, 83–117.

Dissmeyer, N., Rivas, S. and Graciet, E. (2018) Life and death of proteins after protease cleavage: protein degradation by the N-end rule pathway. *New Phytol.* **218**, 929–935.

Dolan, L., Ducket, C.M., Grierson, C., Linstead, P., Schneider, K., Lawson, E., Dean, C., Poethig, S. and Roberts, K. (1994) Clonal relationships and cell patterning of the root epidermis of Arabidopsis. *Development*, 2465–2474.

Ehlert, A., Weltmeier, F., Wang, X., Mayer, C.S., Smeekens, S., Vicente-Carbajosa, J. and Dröge-Laser, W. (2006) Two-hybrid protein-protein interaction analysis in Arabidopsis protoplasts: establishment of a heterodimerization map of group C and group S bZIP transcription factors. *Plant J.* **46**, 890–900.

Finkelstein, R.R., Gampala, S.S.L. and Rock, C.D. (2002) Abscisic acid signaling in seeds and seedlings. *Plant Cell*, **14**, S15–S45.

Fukao, T., Yeung, E. and Bailey-Serres, J. (2011) The submergence tolerance regulator SUB1A mediates crosstalk between submergence and drought tolerance in rice. *Plant Cell*, **23**, 412–427.

Gasch, P., Fundinger, M., Müller, J. T., Lee, T., Bailey-Serres, J., Mustroph, A. (2016) Redundant ERF-VII transcription factors bind to an evolutionarily conserved cis-motif to regulate hypoxia-responsive gene expression in Arabidopsis. *Plant Cell*, **28**, 160–180.

Gelhaye, E., Rouhier, N., Navrot, N. and Jacquot, J.P. (2005) The plant thioredoxin system. *Cell. Mol. Life Sci.* **62**, 24–35.

Gibbs, D.J., Lee, S.C., Isa, N.M. *et al.* (2011) Homeostatic response to hypoxia is regulated by the N-end rule pathway in plants. *Nature*, **479**, 415–418.

Gibbs, D.J., Md Isa, N., Movahedi, M. *et al.* (2014) Nitric oxide sensing in plants is mediated by proteolytic control of group VII ERF transcription factors. *Mol. Cell*, **53**, 369–379.

Gibbs, D.J., Bailey, M., Tedds, H.M. and Holdsworth, M.J. (2016) From start to finish: amino-terminal protein modifications as degradation signals in plants. *New Phytol.* **211**, 1188–1194.

Gibbs, D.J., Tedds, H.M., Labandera, A.-M. *et al.* (2018) Oxygen-dependent proteolysis regulates the stability of angiosperm polycomb repressive complex 2 subunit VERNALIZATION 2. *Nat. Commun.* **9**, 5438.

Graciet, E., Walter, F., Ó'Maoiléidigh, D.S., Pollmann, S., Meyerowitz, E.M., Varshavsky, A. and Wellmer, F. (2009) The N-end rule pathway controls multiple functions during Arabidopsis shoot and leaf development. *Proc. Natl Acad. Sci. USA*, **106**(32), 13618–13623.

Ha, C.V., Leyva-González, M.A., Osakabe, Y. *et al.* (2014) Positive regulatory role of strigolactone in plant responses to drought. *Proc. Natl Acad. Sci. USA*, **111**, 851–856.

Heyman, J., Cools, T., Vandenbussche, F. *et al.* (2013) ERF115 controls root quiescent center cell division and stem cell replenishment. *Science*, **342**, 860–863.

Heyman, J., Cools, T., Canher, B. *et al.* (2016) The heterodimeric transcription factor complex ERF115-PAT1 grants regeneration competence. *Nat. Plants*, **2**, 16165.

Heyman, J., Canher, B., Bisht, A., Christiaens, F. and De Veylder, L. (2018) Emerging role of the plant ERF transcription factors in coordinating wound defense responses and repair. *J. Cell Sci.* **131**, pii: jcs208215.

Hirabayashi, Y., Kanae, S., Emori, S., Oki, T. and Kimoto, M. (2008) Global projections of changing risks of floods and droughts in a changing climate. *Hydrol. Sci. J.* **53**, 754–772.

Hirabayashi, Y., Mahendran, R., Koirala, S., Konoshima, L., Yamazaki, D., Watanabe, S., Kim, H. and Kanae, S. (2013) Global flood risk under climate change. *Nat. Clim. Chang.* **3**, 816–821.

Holman, T.J., Jones, P.D., Russell, L. *et al.* (2009) The N-end rule pathway promotes seed germination and establishment through removal of ABA sensitivity in Arabidopsis. *Proc. Natl Acad. Sci. USA*, **106**, 4549–4554.

Horan, K., Jang, C., Bailey-Serres, J., Mittler, R., Shelton, C., Harper, J.F., Zhu, J.K., Cushman, J.C., Gollery, M. and Girke, T. (2008) Annotating genes of known and unknown function by large-scale coexpression analysis. *Plant Physiol.* **147**, 41–57.

Hsu, F.C., Chou, M.Y., Chou, S.J., Li, Y.R., Peng, H.P. and Shih, M.C. (2013) Submergence confers immunity mediated by the WRKY22 transcription factor in Arabidopsis. *Plant Cell*, **25**, 2699–2713.

Ikeuchi, M., Iwase, A., Rymen, B. *et al.* (2017) Wounding Triggers Callus Formation via Dynamic Hormonal and Transcriptional Changes. *Plant Physiology*, **175**, 1158–1174.

Karimi, M., de Meyer, B. and Hilson, P. (2005) Modular cloning in plant cells. *Trends Plant Sci.* **10**, 103–105.

Klecker, M., Gasch, P., Peisker, H., Dörmann, P., Schlicke, H., Grimm, B. and Mustroph, A. (2014) A shoot-specific hypoxic response of Arabidopsis sheds light on the role of the phosphate-responsive transcription factor PHOSPHATE STARVATION RESPONSE1. *Plant Physiol.* **165**, 774–790.

Koncz, C., Kreuzaler, F., Kalman, Z. and Schell, J. (1984) A simple method to transfer, integrate and study expression of foreign genes, such as chicken ovalbumin and alpha-actin in plant tumors. *EMBO J.* **3**, 1029–1037.

Laloi, C., Mestres-Ortega, D., Marco, Y., Meyer, Y. and Reichheld, J.-P. (2004) The Arabidopsis cytosolic thioredoxin h5 gene induction by oxidative stress and its W-box-mediated response to pathogen elicitor. *Plant Physiol.* **134**, 1006–1016.

Lee, S.C., Mustroph, A., Sasidharan, R., Vashisht, D., Pedersen, O., Oosumi, T., Voesenek, L.A. and Bailey-Serres, J. (2011) Molecular characterization of the submergence response of the *Arabidopsis thaliana* ecotype Columbia. *New Phytol.* **190**(2), 457–471.

León, J., Rojo, E. and Sánchez-Serrano, J.J. (2001) Wound signalling in plants. *J. Exp. Bot.* **52**, 1–9.

Licausi, F., Kosmacz, M., Weits, D.A., Giuntoli, B., Giorgi, F.M., Voesenek, L.A., Perata, P. and van Dongen, J.T. (2011) Oxygen sensing in plants is mediated by an N-end rule pathway for protein destabilization. *Nature*, **479**, 419–422.

Lin, C.C., Chao, Y.T., Chen, W.C. *et al.* (2019) Regulatory cascade involving transcriptional and N-end rule pathways in rice under submergence. *Proc. Natl Acad. Sci. USA*, **116**, 3300–3309.

Liu, Y., Ji, X., Zheng, L., Nie, X. and Wang, Y. (2013) Microarray analysis of transcriptional responses to abscisic acid and salt stress in *Arabidopsis thaliana*. *Int. J. Mol. Sci.* **14**, 9979–9998.

Lorang, J., Kidarsa, T., Bradford, C.S., Gilbert, B., Curtis, M., Tzeng, S.C., Maier, C.S. and Wolpert, T.J. (2012) Tricking the guard: exploiting plant defense for disease susceptibility. *Science*, **338**, 659–662.

Matsuo, M., Johnson, J.M., Hieno, A. *et al.* (2015) High REDOX RESPONSIVE TRANSCRIPTION FACTOR1 levels result in accumulation of reactive oxygen species in *Arabidopsis thaliana* shoots and roots. *Mol. Plant*, **8**, 1253–1273.

Meyer, Y., Vignols, F. and Reichheld, J.P. (2002) Classification of plant thioredoxins by sequence similarity and intron position. *Methods Enzymol.* **347**, 394–402.

Müller, M. and Schmidt, W. (2004) Environmentally induced plasticity of root hair development in Arabidopsis. *Plant Physiol.* **134**, 409–419.

Mustroph, A., Zanetti, M.E., Jang, C.J., Holtan, H.E., Repetti, P.P., Galbraith, D.W., Girke, T. and Bailey-Serres, J. (2009) Profiling translatomes of discrete cell populations resolves altered cellular priorities during hypoxia in Arabidopsis. *Proc. Natl Acad. Sci. USA*, **106**, 18843–18848.

Mustroph, A., Lee, S.C., Oosumi, T., Zanetti, M.E., Yang, H., Ma, K., Yaghoubi-Masihi, A., Fukao, T. and Bailey-Serres, J. (2010) Cross-kingdom comparison of transcriptomic adjustments to low-oxygen stress highlights conserved and plant-specific responses. *Plant Physiol.* **152**, 1484–1500.

Nakano, T., Suzuki, K., Fujimura, T. and Shinshi, H. (2006) Genome-wide analysis of the ERF gene family in Arabidopsis and rice. *Plant Physiol.* **140**, 411–432.

Nishiyama, R., Watanabe, Y., Leyva-Gonzalez, M.A. *et al.* (2013) Arabidopsis AHP2, AHP3, and AHP5 histidine phosphotransfer proteins function as redundant negative regulators of drought stress response. *Proc. Natl Acad. Sci. USA*, **110**, 4840–4845.

Pacifici, E., Polverari, L. and Sabatini, S. (2015) Plant hormone cross-talk: the pivot of root growth. *J. Exp. Bot.* **66**, 1113–1121.

Pacifici, E., Di Mambro, R., Dello Ioio, R., Costantino, P. and Sabatini, S. (2018) Acidic cell elongation drives cell differentiation in the Arabidopsis root. *EMBO J.* **37**, pii: e99134.

Pandey, G.K., Grant, J.J., Cheong, Y.H., Kim, B.G., Li, L. and Luan, S. (2005) ABR1, an APETALA2-domain transcription factor that functions as a repressor of ABA response in Arabidopsis. *Plant Physiol.* **139**, 1185–1193.

Pandey, S.P., Roccaro, M., Schön, M., Logemann, E. and Somssich, I.E. (2010) Transcriptional reprogramming regulated by WRKY18 and WRKY40 facilitates powdery mildew infection of Arabidopsis. *Plant J.* **64**, 912–923.

Park, S.Y., Fung, P., Nishimura, N. *et al.* (2009) Abscisic acid inhibits type 2C protein phosphatases via the PYR/PYL family of START proteins. *Science*, **324**, 1068–1071.

Reichheld, J.-P., Mestres-Ortega, D., Laloi, C. and Meyer, Y. (2002) The multigenic family of thioredoxin h in *Arabidopsis thaliana*: specific expression and stress response. *Plant Physiol. Biochem.* **40**, 685–690.

Riber, W., Müller, J.T., Visser, E.J., Sasidharan, R., Voesenek, L.A. and Mustroph, A. (2015) The greening after extended darkness1 is an N-end rule pathway mutant with high tolerance to submergence and starvation. *Plant Physiol.* **167**, 1616–1629.

Sah, S.K., Reddy, K.R. and Li, J. (2016) Abscisic acid and abiotic stress tolerance in crop plants. *Front. Plant Sci.* **7**, 571.

Sasidharan, R., Hartman, S., Liu, Z., Martopawiro, S., Sajeev, N., van Veen, H., Yeung, E. and Voesenek, L.A.C.J. (2018) Signal dynamics and interactions during flooding stress. *Plant Physiol.* **176**, 1106–1117.

Seki, M., Ishida, J., Narusaka, M. *et al.* (2002) Monitoring the expression pattern of around 7,000 Arabidopsis genes under ABA treatments using a full-length cDNA microarray. *Funct. Integr. Genomics*, **2**, 282–291.

Song, L., Huang, S.C., Wise, A., Castanon, R., Nery, J.R., Chen, H., Watanabe, M., Thomas, J., Bar-Joseph, Z. and Ecker, J.R. (2016) A transcription factor hierarchy defines an environmental stress response network. *Science*, **354**, pii: aag1550.

Stahl, D.J., Kloos, D.U. and Hehl, R. (2004) A sugar beet chlorophyll a/b binding protein promoter void of G-box like elements confers strong and

leaf specific reporter gene expression in transgenic sugar beet. *BMC Biotechnol.* **4**, 31.

Sweat, T.A. and Wolpert, T.J. (2007) Thioredoxin h5 is required for victorin sensitivity mediated by a CC-NBS-LRR gene in Arabidopsis. *Plant Cell*, **19**, 673–687.

Tsai, K.J., Lin, C.Y., Ting, C.Y. and Shih, M.C. (2014) Ethylene plays an essential role in the recovery of Arabidopsis during post-anaerobiosis reoxygenation. *Plant, Cell Environ.* **37**, 2391–2405.

van Veen, H., Vashisht, D., Akman, M. *et al.* (2016) Transcriptomes of eight *Arabidopsis thaliana* accessions reveal core conserved, genotype- and organ-specific responses to flooding stress. *Plant Physiol.* **172**, 668–689.

Vicente, J., Mendiondo, G.M., Movahedi, M. *et al.* (2017) The Cys-Arg/N-end rule pathway is a general sensor of abiotic stress in flowering plants. *Curr. Biol.* **27**, 3183–3190.e4.

Vicente, J., Mendiondo, G.M., Pauwels, J. *et al.* (2018) Distinct branches of the N-end rule pathway modulate the plant immune response. *New Phytol.* https://doi.org/10.1111/nph.15387.

Walton, A., Stes, E., Cybulski, N. *et al.* (2016) It's time for some "site"-seeing: novel tools to monitor the ubiquitin landscape in *Arabidopsis thaliana*. *Plant Cell*, **28**, 6–16.

Wang, Z., Cao, G., Wang, X., Miao, J., Liu, X., Chen, Z., Qu, L.J. and Gu, H. (2008) Identification and characterization of COI1-dependent transcription factor genes involved in JA-mediated response to wounding in Arabidopsis plants. *Plant Cell Rep.* **27**, 125–135.

Wang, C., Ding, Y., Yao, J., Zhang, Y., Sun, Y., Colee, J. and Mou, Z. (2015) Arabidopsis Elongator subunit 2 positively contributes to resistance to the necrotrophic fungal pathogens *Botrytis cinerea* and *Alternaria brassicicola*. *Plant J.* **83**, 1019–1033.

Wehner, N., Hartmann, L., Ehlert, A., Böttner, S., Oñate-Sánchez, L. and Dröge-Laser, W. (2011) High-throughput protoplast transactivation (PTA) system for the analysis of Arabidopsis transcription factor function. *Plant J.* **68**, 560–569.

Weits, D.A., Giuntoli, B., Kosmacz, M., Parlanti, S., Hubberten, H.M., Riegler, H., Hoefgen, R., Perata, P., van Dongen, J.T. and Licausi, F. (2014) Plant cysteine oxidases control the oxygen-dependent branch of the N-end-rule pathway. *Nat. Commun.* **5**, 3425.

Weits, D.A., Kunkowska, A.B., Kamps, N.C.W. *et al.* (2019) An apical hypoxic niche sets the pace of shoot meristem activity. *Nature*, **569**, 714–717.

White, M.D., Klecker, M., Hopkinson, R.J. *et al.* (2017) Plant cysteine oxidases are dioxygenases that directly enable arginyl transferase-catalysed arginylation of N-end rule targets. *Nat. Commun.* **8**, 14690.

White, M.D., Kamps, J.J.A.G., East, S., Taylor Kearney, L.J. and Flashman, E. (2018) The plant cysteine oxidases from *Arabidopsis thaliana* are kinetically tailored to act as oxygen sensors. *J. Biol. Chem.* **293**, 11786–11795.

Wu, F.-H., Shen, S.-C., Lee, L.-Y., Lee, S.-H., Chan, M.-T. and Lin, C.-S. (2009) Tape-Arabidopsis Sandwich - a simpler Arabidopsis protoplast isolation method. *Plant Methods*, **5**, 16.

Yeung, E., van Veen, H., Vashisht, D. *et al.* (2018) A stress recovery signaling network for enhanced flooding tolerance in *Arabidopsis thaliana*. *Proc. Natl Acad. Sci. USA*, **115**, E6085–E6094.

Yoshida, S., Ito, M., Callis, J., Nishida, I. and Watanabe, A. (2002) A delayed leaf senescence mutant is defective in arginyl-tRNA: protein arginyltransferase, a component of the N-end rule pathway in Arabidopsis. *Plant J.* **32**, 129–137.